Red Queen evolution driven by asymmetric competition.

Jostein Starrfelt

Cand. scient. thesis

Centre for Ecological and Evolutionary Synthesis
Department of Biology
University of Oslo

2006

Forord.

Hovedfaget startet plutselig for lenge siden, og jeg hang meg på et løselig definert prosjekt Jens Ådne hadde fikset hos Nils Christian Stenseth. Glenn-Peter Sætre ble hyret inn som andremann og har vært den som har hjulpet meg mest gjennom evolusjonsteoriens fulle bredde. Han er høyt verdsatt hva angår fag, ikke-fag og ikke minst fullstendig ikke-faglige musikkseanser.

Det har til tider gått både trått og seint, heldigvis ikke hele tiden, og hva jeg har lært…

Det er mange som fortjener takk, mest av alle Jens Ådne, som har vært en utrolig inspirator, et oppkomme av biologiske fakta i tillegg til en habil musiker og venn. Uten deg hadde jeg nok ikke gjort det jeg gjør i dag. Av ren faglig karakter også noen andre enn Glenn-Peter og takke; Øistein Holen for tips og hjelp, Thomas Svennungsen for det samme, og selvsagt til Nils Christian for å ha dannet et av de mest inspirerende og faglig stimulerende miljøer jeg kan se for meg å være som student eller forsker. Andre faglige og ikke-faglige takk rettes til en hel haug med mennesker som jeg har nytt livet sammen med på bio, ikke minst til tidligere og nåværende kverulanter og nikkedukker på Centre for Scientific and Cultural Synthesis. Av de som har lengst fartstid er selvsagt Ingebof , Petter, Per, Ragnar og Irja, alle fantastiske mennesker jeg har solet meg i glansen av gjennom de siste årene, men de sist ankomne, Kjetil, Torbjørn, Gry og Kristina takkes også. I tillegg rettes en dypfølt og inderlig takk til den av tvillingene som sørget for at det kom et fußball-bord inn på senteret, det har vært til en så umåtelig glede og oppkvikker i de øyeblikkene en klarer å rive seg fra arbeidet. Alle mine venner gjennom opphavssted og ikke-fag, Ådne, Jørgen, Øyvind*2, Lars og flere, takkes for å gjøre Oslo til en fredens og bedagelighetens by å bo i for en landsens gutt som meg.

Sist, men absolutt ikke minst, takk til Ingeborg, for å trekke meg høyere opp på lykkeskalaen.

Blindern, 23/03/06

Abstract.

The Red Queen hypothesis states that biological entities rather than abiotic factors constitute the larger part of the selective environment experienced by individual organisms, and that species as a consequence undergo continual evolution. Such non-stationary evolutionary dynamics can exist on a fine evolutionary scale, where a constant number of co-evolving species engage in fixed ecological interactions. Phenotypic models of evolution can reflect such continuous evolution through limit cycles in the evolution of traits. Here a dynamic phenotypic model of trait evolution under asymmetric intra- and interspecific competition is presented and analyzed. The model comprises two species or populations competing for resources, where the value of a trait, such as body size, of the interacting individuals determines the competitive effects. A cost for having a trait size different from a defined ecological optimum (i.e. optimal in the absence of competition) is included. The degrees of intra- and inter-specific asymmetry affect evolutionary dynamics in very different ways. The model exhibits Red Queen dynamics in some parts of the investigated parameter space. However, evolutionary limit cycles only occur when there is a certain degree of asymmetry in the inter-specific competitive interactions and when the two populations have different rates of evolution. A shortcut for finding equilibria where such continual dynamics can be achieved in adaptive dynamics models is also presented. This shortcut applies weak convergence stable equilibrium points in any adaptive dynamics model with two species with one evolving trait each.

1. Introduction.

1.1 The Red Queen hypothesis.

The Red Queen hypothesis was put forth by Van Valen (1973) and was based on interpretation of paleontological data. His analysis suggested that the longevity of any taxon did not affect the probability that species within the taxa would go extinct. This led him to the hypothesis that all species are continuously evolving and coined the term Red Queen evolution to describe this non-stationary evolutionary dynamics. The name comes from Lewis Carroll's *Behind the looking glass* (Carroll 1872), where the red queen says to Alice that '…it will take all the running you can do, just to stay in the same place'.

The Red Queen hypothesis is one out of very few dealing with large-scale evolutionary patterns and processes, and has been investigated from different biological approaches. One of the first thorough model-approaches to investigate the hypothesis was done by Stenseth and Maynard-Smith (1984), focusing on community patterns. Their model distinguishes between three timescales: i) The ecological time scale, where the variables are the species abundances; ii) The gene frequency time scale, where the number of species and the nature of their interactions are constant; and iii) The speciation-extinction timescale. Their analysis suggested that in the absence of environmental changes, ecosystems are expected to approach one of two possible states. One is a stationary state, in which ecosystems are stable in number of species and with few evolutionary changes. The other is the Red Queen state, in which there is a steady state characterized by a uniform rate of evolution, speciation and extinction. Accordingly, the model poses the possibilities of two different regimes in the history of evolution under stable environmental conditions: that of stasis or of continual, non-stationary evolutionary dynamics. If most species are continuously evolving, this may be reflected in the fossil-record (which was what led Van Valen to put forward his hypothesis), although not necessarily so, because there are many evolvable traits, such as cellular processes and behavioral traits, that are not fossilized. The hypothesis is often put up against that of Vrba on turnover-pulses (1993) and other "Court Jester hypotheses" (Barnosky 2001), which suggest that biological communities are fairly stable in composition and have

stable rates of extinction and immigration/speciation when the environment is stable, and undergo a turnover-pulse when large-scale climatic or tectonic changes occurs. The debate is still ongoing, particularly with respect to evolution of mammal communities (Vrba 1993, Alroy 1996, Alroy et al. 2000, Raia et al. 2005)

The interpretation of the Red Queen hypothesis in the above mentioned debate relates to whether biological communities, on the evolutionary timescale (i.e. with respect to extinction and speciation), are mainly shaped by biological interactions or by external forcing. However, the hypothesis can also be interpreted at a finer scale, in terms of evolution of co-evolving species. In the latter view, Red Queen dynamics can be consistent with Vrba's turnover-pulses. This is because in the absence of external changes, a species might still undergo continual evolution in adapting to other species with which it interacts ecologically. This can have an effect on turnover-rates if such evolution leads to recurrent extinction and speciation. However, one can also envision continual evolution without changes in species composition of an ecological system. Such type of non-stationary dynamics would correspond to Red Queen evolution on the second timescale as defined by Stenseth and Maynard-Smith (1984), the 'gene-frequency time-scale' where the number of species and the nature of their interactions are constant. In this latter view of the Red Queen, investigations of conditions for lack of evolutionary stasis in phenotypic models that incorporate frequency-dependent fitness of co-evolving species can potentially yield fruitful insights.

1.2 Red Queen evolution on the 'gene frequency' time scale.

Investigations of Red Queen evolution in systems of fixed interactions have in many cases not assumed a fixed number of coevolving species. Most of the models constructed to address the possibilities of non-stationary dynamics on the time scale of fixed interactions are of predator-prey, parasite-host or general exploiter-victim type (Marrow et al. 1992, Dieckmann et al. 1995, Gavrilets 1997, Martins 2000, Gandon 2002, Loeuille et al. 2002, Dercole et al. 2003, Kisdi and Liu 2006). In most exploiter-victim systems such continual dynamics is fairly common. Competition has also been studied (Dawkins and Krebs 1979, Parker 1983, Abrams and Matsuda 1994, Matsuda and Abrams 1994, Law et al. 1997, Kisdi and Geritz 2001, Kisdi 2004), also on a larger scale relating to

taxon-cycles (Taper and Case 1992) or to other patterns of fluctuating diversity (Kisdi 1999, Doebeli and Dieckmann 2000, Kisdi and Geritz 2003). Most of these models of competition are either focused on intra-specific competition or with varying number of interacting species.

Competition is a ubiquitous phenomenon in natural communities, and thus the evolutionary consequences of different competitive interactions both within and between species are of interest. Competition can be characterized by the actual way the interactions are undertaken; in exploitative competition the detriment for one individual is due to other individuals consuming the same resources, whereas in interference competition the individuals directly interact in competition over some resource. Competitive interactions are said to be asymmetric when the fitness effect of the interaction differs between the individuals. Asymmetries in competitive interactions are likely to exist in both types of competition, but are probably more predominant in direct interference competition (Persson 1985). Competitive asymmetries includes direct contests where the larger individual wins with a higher probability (Cluttonbrock et al. 1979) or gets a larger share of the resource (see e.g. Schwinning and Weiner (1998)). Asymmetries are also prevalent in the competition for territories (Robinson and Terborgh 1995) and appears both within and between species (Persson 1985, Alatalo and Moreno 1987, Morin and Johnson 1988, Robinson and Terborgh 1995). The degree of asymmetry in competitive interactions has potential to greatly affect the evolution of traits determining competitive ability, and has therefore been studied to a certain extent. However, to my knowledge, the only model of evolutionary dynamics with focus on co-evolution of persistent populations (except for co-evolution as a result of evolutionary branching or re-occurring invasions) engaging in asymmetric competitive interactions was published by Law et al. (1997). Their model comprised two species/populations where one evolvable trait in each population influenced the basal mortality of the populations as well as determined the effect of the competitive interactions. The traits were interpreted as body sizes, as they are of importance in competitive interactions (Weiner 1990). The model showed that asymmetry (i.e. unequal division of fitness effects) in competitive interactions can give rise to several more equilibrium points in

addition extinction of one of the species. They also presented one example of limit cycle in the system. One could, however, question their choice of mathematical representations of the biological interactions. One would expect that the degree of competition between individuals and populations should diminish with increasing differences in trait-values between the competitors, as larger differences in body size could correspond to less overlap of resource utilization. This was not assumed in their model, where the interaction coefficient was as depicted in figure 1. Another potential problem is that they defined every trait-value below zero as impossible and just used a linear cost-function, although they introduced a suggestion on how one could transform body sizes. One should, however, expect there to be an optimal body size defined by the abiotic environment in the absence of competition, and a region of body sizes around that optimum. A model describing the evolutionary dynamics of asymmetric competition where these objections are taken into account is therefore needed.

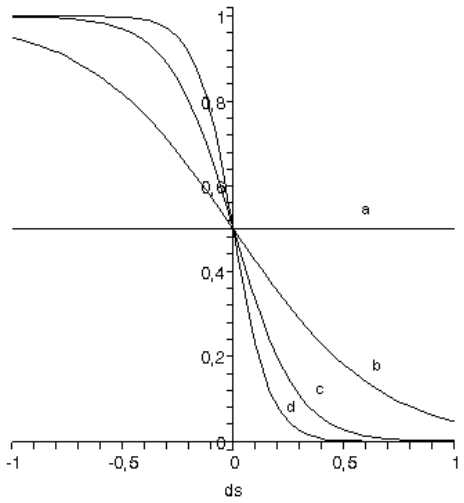

Figure 1. The competitive interaction function in Law et al. (1997) with increasing levels of asymmetry. The first axis represents difference in trait value for the two individuals and the second denotes the ecological impact of the competitive interaction. From a – no asymmetry to d – strong asymmetry and a < b < c < d in level of asymmetry.

1.3 Purpose

The purpose of the model presented here is to model biological competition, take the above objections to the model by Law et al. (1997) into account, and to evaluate under

what conditions a coevolutionary model of competition will exhibit evolutionary limit cycles. The model consists of two species or populations that compete for a common resource. The parameters of interest are first and foremost the degree of asymmetry in the competitive interaction, but other parameters will also be briefly analyzed. Asymmetry is unequal division of competitive impacts between the two entities engaging in competitive interactions and is of particular interest because of the probable predominance of asymmetric competition in contrast to symmetric in nature. (Lawton and Hassell 1981, Connell 1983, Schoener 1983, Weiner 1990)

In addition to a deterministic model of evolutionary change, an individual-based model and a monomorphic stochastic model (Dieckmann and Law 1996) was constructed (see appendix 2 and 3 for details). The main reason for including these additional models was to investigate whether solutions of the deterministic approximation would be validated with simulations in which some of the assumptions are lifted. Another reason was to evaluate if the occurrence of limit cycles in the deterministic approximation would be evident also in a polymorphic stochastic model, where the possibilities of such cycles could be affected by the fact that populations are polymorphic with a certain degree of phenotypic variance. A deterministic approximation of a cycle can for instance be of small amplitude and individual-based simulations can shed light on the dynamics in the system if the variation within a population is larger than the amplitude.

2. The model.

2.1. The framework.

One of the frameworks for dynamic modeling of phenotypic evolution developed in the last decades is loosely termed adaptive dynamics. The main contribution to the development of the approach was that of invasion-fitness as the long term per capita growth rate of a (potential) mutant in a system defined by existing phenotypes called residents (Metz et al. 1992). The derivative of the invasion-fitness with respect to the mutant is then used as a fitness-gradient in a dynamical system of monomorphic population(s) as an approximation of evolution by small mutational steps. This approximates the mean path of many realizations of a stochastic mutation-selection process, and is termed the canonical equation of adaptive dynamics (Dieckmann 1996, Marrow et al. 1996).

The models of adaptive dynamics are especially suited for investigating the Red Queen hypothesis due to the possibilities of deriving evolutionary models from ecological models, such that ecological parameters are explicitly incorporated into the evolutionary system. In the adaptive dynamics literature, the term Red Queen dynamics is used to describe two qualitatively different types of continual evolution. One is branching-extinction cycles (Geritz et al. 1997, Geritz et al. 1998, Kisdi 1999, Doebeli and Dieckmann 2000, Kisdi et al. 2001, Bowers et al. 2003) where evolution is non-stationary in the sense of lineages branching into several populations or species, with following Darwinian extinction (Webb 2003) and reoccurring branching. The other form is the existence of limit cycles in the adaptive trait-space (Dieckmann et al. 1995, Abrams and Matsuda 1997a, 1997b, Law et al. 1997) where evolution never halts due to lack of stable point attractors.

2.1.1. Properties of evolutionary singular strategies.

The possible stationary outcomes of a one-dimensional adaptive dynamics model can be characterized by certain analytical properties (Geritz et al. 1998). The points where the fitness gradient disappears can be characterized by the double-derivatives of the invasion-

fitness with respect to the mutant's and the resident's phenotype. Following Geritz et al. (1998), properties of evolutionary singular strategies can be classified into eight different categories, depending on the values of the following mathematical properties, evaluated at points where the selection gradient disappears called a singular point:

(a) $\frac{\partial^2}{\partial s_i^{\,2}} f\left(s_{mut|i}, s\right)\Big|_{s_{mut|i}=s_i}$ (b) $\frac{\partial^2}{\partial s_{mut|i}^{\,2}} f\left(s_{mut|i}, s\right)\Big|_{s_{mut|i}=s_i}$

Property of the singular strategy	Mathematical criteria
ESS stability, δ – stability	(b) < 0
Convergence stability, *m* –stability	(a) – (b) > 0
Singularity can spread	(a) > 0
Nearby dimorphisms	(a) + (b) > 0

Table 2. Properties of singular strategies and their characterization, after Geritz et al. (1998)

Here $f\left(s_{mut|i}, s\right)$ represents the fitness of an initially rare mutant with phenotype $s_{mut|i}$ in a system defined by the vector *s*, denoting the phenotypes of the residents.

The delineation of the two first properties as independent was of great importance in the extension of the traditional static definition of ESS's (Evolutionarily Stable Strategies). Without both ESS stability and convergence stability, an ESS in the old sense is not attainable by small mutational steps. The original distinction of the two first properties is δ-stability and *m*-stability from Taylor (1989), elaborated by Christiansen (1991), due to earlier work by Eshel and Motro (Eshel and Motro 1981, Eshel 1983). One of the conclusions from this distinction is the appearance of convergence stable, not ESS stable points of attraction. If these singular strategies also fulfill the last criteria with nearby dimorphisms, it corresponds to a branching point; a point where the population might split into two populations with different trait-values (Geritz et al. 1997, Geritz et al. 1998, Kisdi 1999, Doebeli and Dieckmann 2000, Geritz and Kisdi 2000). This can in some cases also lead to cycles of branching and extinction of one of the morphs, followed by branching events, one form of Red Queen dynamics (Kisdi et al. 2001, Dercole 2003) in such models. The application from Geritz et al.(1998) only applies to one-dimensional models, but some of the conditions have also been extended to multidimensional models (Leimar 2002). Leimar (Leimar 2002) introduces the concept of strong convergence

stability as a multidimensional extension of convergence stability. In the case of non-correlated traits in several dimensions (as is the case if there is only one trait in every population in the model) strong convergence stability implies asymptotic stability of the dynamical system and convergence stability for all of the populations. This concept is needed due to the fact that an attractor in the dynamical system must be convergence stable for some of the evolving populations but not necessarily all. If an attractor exhibits strong convergence stability it is however convergence stable for all populations. Attractors can thus have strong convergence stability ($a-b > 0$ for all populations) or weak convergence stability ($a-b>0$ for one population). Note, however, that these criteria only apply to evolutionary singular strategies that are contenders of the final resting stops for evolution and thus that the existence of limit cycles in the system can not be characterized by the use of these criteria.

2.1.2. The applicability of adaptive dynamics models.

Most limitations of models lie in their assumptions, and the derivation of the canonical equation together with the assumptions about the particular system under investigation all limit its applicability to natural systems. As in other phenotypic models haploid and asexual reproduction is assumed, which clearly only applies to a limited set of organisms. On the other hand, numerical explorations of sexually reproducing individual-based models has in several cases shown to follow very similar dynamics as the haploid, asexual ones (Dieckmann and Doebeli 1999, Geritz and Kisdi 2000). Other limitations include those of small mutational steps, general mutation-limited evolution (i.e. fixation of one mutant before another appears) and decoupling of ecological and evolutionary timescales. The assumptions and therefore limitations of the adaptive dynamics models are still under debate, and the adequacy of adaptive dynamics as models for evolution is continuously questioned (see Waxman and Gavrilets (2005) with replies and further comments in same issue).

In spite of its limitations, adaptive dynamics models have a solid basis, as the approximation can be derived from stochastic mutation-selection processes and also from a starting point in quantitative genetics (Iwasa and Pomiankowski 1991, Taper and Case 1992, Abrams et al. 1993a, Abrams et al. 1993b, Dieckmann et al. 1995, Marrow et al.

1996). Another strength of the approach is the fact that the framework has four distinct types of models, with different assumptions and degrees of realism, three of which are utilized in this thesis. It also includes both frequency- and density-dependence in the evolution of traits, and it is fairly easy and straightforward to construct dynamic models for very different ecological scenarios.

2.2. A model of asymmetric competition.

The basic scenario here is a coevolutionary model of competition, where two populations assumed to be different species, engage in competitive interactions. Each population consists of individuals having one trait, which we may think of as body size, which undergoes evolution. The trait sizes has primarily two effects, they affect the impact of competition; it is assumed that differences in trait sizes between two interacting individuals determines the mortality effect on both. There is also a cost associated with trait size, and an optimal trait size in the absence of competition is defined. Having a larger or smaller trait size than the optimum incurs some cost through increased mortality risk. The growth rate of the populations being monomorphic for one trait size can then be expressed as functions of these relationships if one includes a birth rate, here assumed to be independent of the trait size. The main focus of investigation is the degree of asymmetry in the competitive interactions, where increasing asymmetry means that the individuals or populations with the smaller trait size have disproportionately larger mortality risk due to competition than those having larger trait size. First, the functions describing the relationship between trait size and mortality risks are introduced; then a population dynamic system is constructed, and finally an evolutionary dynamical model is derived from the system. The dynamical model is interpreted as an approximation to several runs of the stochastic models presented at the end of this section.

2.2.1. Individual interactions.

2.2.1.1. The competition function alpha

The competition function alpha describes the level of competition between two individuals, as a function of the individuals' trait-values (denoted s_i and s_j) and the degree of asymmetry (denoted $k_{i,j}$). The trait-values can, as suggested above, be interpreted as body size of the individuals, which is often important in competitive interactions, but can

represent any phenotypic trait that can be transformed into a scalar value and is of importance in the competitive interaction (such as degree of armament, weight, or costly signals of strength). The numerical value of the function is assumed to translate into probabilities of dying per encounter per unit time. Per encounter can mean direct encounter as in interference competition, or imagined encounter due to encountering a resource that already has been utilized by another individual. Increasing levels of asymmetry means that the impact of the interaction is divided differently between the two individuals differing in trait-values, with lack of asymmetry corresponding to an equal effect. The competition function (I) reflects certain desired properties; equal effect on both individuals if they have the same scalar trait value independent of the level of asymmetry; decreasing effect when the difference in trait-values increases (unlike Law et al. (1997)); an increase in the level of asymmetry skews the function in the opposite direction of the asymmetry; and finally, the sum of effects of the interaction is the same for the same difference in trait-values, irrespective of the level of asymmetry:

$$\alpha\left(s_i, s_j, k_{i,j}\right)/\gamma = \frac{\exp\left(-\left(s_i - s_j\right)^2\right)}{1+\exp\left(k_{i,j}\cdot\left(s_i - s_j\right)\right)} \qquad \text{(I)}$$

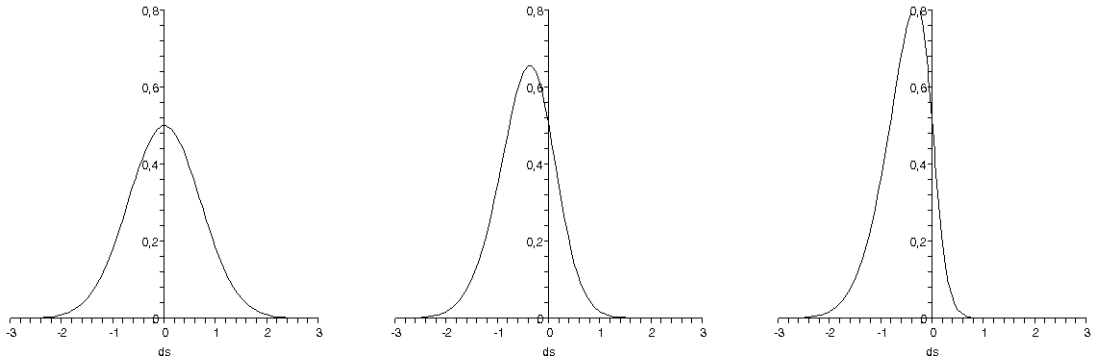

Figure 2..Interaction coefficient α for different degrees of asymmetry. The x-axis is the difference in trait-values for the two competing individuals/populations. a) $k_{i,j} = 0$. b) $k_{i,j} = 3$. c) $k_{i,j} = 7$.

If one sets the trait values equal, the level of competition calculates to the numerical value of ½, as it will for all levels of asymmetry. One can also easily see that the effect of the interaction will decrease for increasing difference in trait-values, as the numerator depends on the exponential of the negative squared difference in trait value. That the

function reflects the wanted property of asymmetry is accomplished by the denominator, and is most easily seen graphically, in figure 2. The parameter γ has the unit $time^{-1}$ and specify the temporal aspect of the interaction and thereby scales the population sizes.

2.2.1.2. The cost function delta

Trait sizes cannot evolve *ad infinitum* and there is likely a cost for having larger values of a trait such as body size. This cost could represent lower fecundity or higher mortality risk, and must be incorporated in the model. We here assume that there is an optimal trait size, and that deviations from that optimal size incur increased mortality risks. Thus, the cost-function here is of second-order to make sure that there is an optimal trait size (in absence of competition), accomplished by setting the appropriate parameters into the function:

$$\delta(s_i) = c_1 - c_2 \cdot s_i + c_3 \cdot s_i^2 \qquad \text{(II)}$$

This function will have a parabola-shape with a minimum at $c_2/(2 \cdot c_3)$, when we assume all parameters to be positive.

The cost function, together with the intrinsic birth rate, β_i, could be viewed as the resource that the populations consume, and therefore defining an alike to the carrying capacity or maximum attainable resource, dependent on the trait value. In that case any difference in β_i's can be interpreted as a difference in the ability to utilize the resource, irrespective of the evolvable trait. One could also imagine different cost-functions for the different populations, but here the parameters used are equal for both.

2.2.2. Population dynamics

The population dynamics of the system can be derived using the alpha-function above if we assume that individuals encounter each other at random. Then, the alpha-function together with the mortality risk $\delta(s)$ translates into net rates of increase (or decrease) for the whole population of individuals. I here assume that the populations are monomorphic for one trait size. The functions can then be incorporated in a model of Lotka-Volterra type (sensu latu);

$$\frac{dN_i(t)}{dt} = N_i(t)\cdot f(\mathbf{s},\mathbf{N}) = N_i(t)\cdot\left(\beta_i - \delta(s_i) - \sum_{j=1,2} c_{i,j}\cdot\alpha(s_i,s_j,k_{ij})\cdot N_j(t)\right) \qquad \text{(III)}$$

Here the change in size of a population *i* is a product of the population size at time *t* and a function for the population's growth rate, which again depends on the trait values of the populations (***s***, a vector consisting of two traits, s_1 and s_2) and the population sizes (***N***, indicating the vector of population sizes). This function (from now on referred to as the growth function) consists of several parameters where β_i is the intrinsic birth rate of population *i*; the function δ, which corresponds to basal mortality and which depends on the trait value of the focal population only; and two terms describing the competitive interaction within and between the populations. The cost-function is here assumed to translate into rates of mortality as a function of the trait size of the populations. The interaction term has a scaling factor $c_{i,j}$ which scales the effect of an inter-specific versus an intra-specific interaction. This scaling factor is used to allow an interaction to have a stronger effect within a population than between populations, as might be the case when the ecology of the two species differs to some extent. It is important to distinguish the type of asymmetry in the model from the more traditional ecological way of interpreting asymmetry, where asymmetry simply reflects differences in the extent populations affect each other in population dynamics (i.e. differences in the full term $c_{i,j}*\alpha(s_i, s_j, k_{i,j})$). Here the degree of asymmetry in addition to the scaling factors $c_{i,j}$ will determine the impacts.

2.2.3. The canonical equation.

To derive the canonical equation(s) of adaptive dynamics (Dieckmann and Law 1996, Geritz et al. 1998) one introduce a mutant in the dynamic system and define fitness as the long term per capita growth rate of a (potential) mutant invader (Metz et al. 1992). The growth function (invasion fitness) for the mutant invader will then be

$$f(s_{mut},\mathbf{s}) = \beta_i - \delta(s_{mut}) - \sum_{j=1,2} c_{i,j}\cdot\alpha(s_{mut},s_j,k_{ij})\hat{N}_j(s) \qquad \text{(IV)}$$

Here the constants in the function with subscripts (i.e. β_i and $c_{i,j}$) are equal to the corresponding constants of the population where the mutant appears. As is evident from the interaction term we here make one of the fundamental assumptions in adaptive dynamics theory; that the mutant itself does not initially affect the environment in which

it appears. We only calculate the interaction between the mutant and the two resident populations, and how that will affect the initial per-capita growth rate of a potential mutant (it does not initially interact with itself). Thus the environment is completely determined by the resident populations and their trait-values. We also assume that the population dynamics has reached its attractor since we evaluate at the equilibrium population sizes of the two residents, $\hat{N}(s)$, which implies a decoupling of ecological and evolutionary timescales. Thus, the invasion fitness only depends on the resident trait-values which determine the equilibrium population sizes. This function is often called the invasion fitness. We assume that whenever this evaluates to a positive value the mutant will invade and replace the resident population in which it appeared.

If we make the assumption that the two types (that is mutant and resident) cannot coexist in the same population and in addition have infinitesimally small mutational steps (invasion of new types is only possible in the immediate vicinity of the resident trait), we can derive the fitness gradient. This will be the mutant's growth function differentiated with respect to the mutant's trait-value and substituting for the trait-value of the population in which it appears.

$$\frac{\partial}{\partial s_{mut|i}} f_i\left(s_{mut|i}, s\right)\Big|_{s_{mut|i}=s_i} = \lim_{s_{mu|i}-s_i \to 0}\left(\frac{f_i\left(s_{mut|i}, s\right) - f_i\left(s_i, s\right)}{s_{mut|i} - s_i}\right) \qquad \text{(V)}$$

Here $s_{mut|i}$ is the trait-value of the mutant appearing in population *i.* Since we assume that the resident populations have reached their equilibrium sizes, $f_i(s_i,s)$ is zero. This selection derivative (or fitness gradient) is used in a deterministic dynamical system, as it describes the direction of evolution of the trait values in the limit of small mutational steps.

$$\frac{\partial s_i(t)}{\partial t} = \kappa_i\left(s_i\right) \cdot \frac{\partial}{\partial s_{mut}} f\left(s_{mut}, \mathbf{s}\right)\Big|_{s_{mut}=s_i} \qquad \text{(VI)}$$

Here the term $\kappa_i(s_i)$ is the parameters that scale the rate of evolution, and consists of biologically meaningful terms as follows;

$$\kappa\left(s_i\right) = \frac{1}{2} \cdot \mu_i \cdot \sigma_i^2 \cdot \hat{N}_i(s) \qquad \text{(VII)}$$

Here the ½ term arises from the assumption that half of the mutations that appear will be selectively disadvantageous (i.e. have negative invasion fitness), μ_i is the mutation rate, σ_i^2 is the mutational variance and $\hat{N}_i(s)$ is the equilibrium population size of population i as a function of the trait-values.

2.2.4. The monomorphic stochastic and polymorphic stochastic models.

In addition to the deterministic approximation above I constructed two stochastic models, one individual-based and one population-based simulation model, to validate solutions of the deterministic approximation. Evolution is not a deterministic process, and the stochasticity in individual deaths, births and more importantly the randomness of mutations can be taken into account in such stochastic model. An individual-based model will also exhibit some variation of phenotypes within populations, absent in the deterministic approximations, where populations are assumed to be monomorphic. The functions (α and δ) and β_i can map and be scaled such that an individual's trait (together with all other traits in the populations) translates into probabilities for giving rise to a new individual or to die. To construct an individual-based model of the system, one also needs to incorporate mutation probabilities and the distribution of mutations. A birth-event is followed by a mutation of the trait value of the focal individual with probability μ_i, and is drawn from a normal distribution with zero mean and variance σ_i^2. After every event all probabilities are recalculated. In this model both the ecological and the evolutionary dynamics are emergent. Further details of the individual-based model are given in appendix 1.

For construction of the other stochastic model the invasion fitness (eq. IV) of a mutant is used together with the mutational distribution. In this simulation model both populations are assumed to be monomorphic and the invasion fitness together with the mutational distribution determines probabilities for transitions to other trait-values in the vicinity of the resident. Here we assume that there is a separation of time scales such that the populations have reached their population dynamical attractor before any trait-transition will occur. Therefore the model will only have emergent evolutionary dynamics, while

the ecological dynamics are neglected. Further details of the population-based model are given in appendix 2.

3. Analysis of the model.

3.1 Regions of coexistence

Since we are interested in the coevolution of two populations we are restricted to a subset of the Cartesian plane $S = s_1 * s_2$ in which both populations have non-zero and positive population sizes. The isoclines defining this subset can be found by solving the resident population model (III) for the population sizes. There is only one solution with two positive population sizes. With two populations, the population sizes are dependent on every parameter and variable in the resident model (III). In addition to the presence of β and δ there is an augmenting term arising from the interaction with the other population. The subspace of S where both populations are non-zero and positive, S_c, requires that the following inequality is met:

$$S_c = \{s \in S | N(s) > 0\} \Rightarrow \frac{\beta_i - \delta(s_i)}{c_{i,i} \cdot \alpha(s_i, s_i, k_{i,i})} < \frac{\beta_j - \delta(s_j)}{c_{j,i} \cdot \alpha(s_j, s_i, k_{j,i})} \qquad \text{(VIII)}$$

In absence of competition, the region of existence (or equivalently the trait-values for zero population size in absence of competition) is defined by β and the δ-function, which again yields;

$$N_i(s_i) = 0 \rightarrow s_i \in \frac{c_2}{2 \cdot c_3} \pm \frac{\sqrt{c_2^2 + 4 \cdot c_3 \cdot \beta_i - 4 \cdot c_3 \cdot c_1}}{2 \cdot c_3} \qquad \text{(IX)}$$

So, as the first term describes the optimum trait-value according to the delta-function, the second term describes the width of the region of viable trait-values s_i.

If we substitute the values for interactions within a population ($\alpha(s_i, s_i, k_{i,i}) = ½$) and choose values for scaling the effect of an interaction between and within the populations so that a population always affects itself more than the other (to make the inequality VIII hold in a larger subset of S), $c_{i,i} = 2$, $c_{i,j} = 1, i \neq j$, we get the following expression for the equilibrium population sizes;

$$\hat{N}_i = \frac{\beta_i \cdot \gamma - \delta(s_i) \cdot \gamma - \alpha(s_i, s_j, k_{i,j}) \cdot (\beta_j - \delta(s_j))}{(\gamma^2 - \alpha(s_i, s_j, k_{i,j}) \cdot \alpha(s_j, s_i, k_{j,i}))} \quad \text{(X)}$$

This only applies to the monomorphic stochastic and deterministic model, as the individual-based model will have emergent population sizes and a very stochastic representation of those sizes.

From equation X it is obvious that the parameter γ scales the population sizes (it is a part of the α-function), as its square is a part of every term in the denominator and it is part of every term in the numerator. If there is only one population, its size is defined only by the intrinsic birth rate β_i, the value of the cost function δ, and γ. Note that this does not mean that there is no competition acting within the population, only that we have defined competition to have a numerical value of 2*½ =1 for interacting individuals (or populations) with the same trait-value.

We then have an expression for the equilibrium population sizes as a function of the trait-values. The expressions involved are fairly complex and are not solved for *s* analytically, but I use numerical computations to find the subset in which both populations have positive sizes. It is only within this region we can have coevolution, and evolution out of this region will in this model correspond to a Darwinian extinction (Webb 2003).

Since the region of coexistence depends on one of the parameters of interest, namely the degree of asymmetry, I explore the effect of changing the level of asymmetry on the size and shape of the region of coexistence. For the analysis to be simplified I use a baseline-scenario throughout for comparison. The parameter settings for this scenario applies and are as follows if not otherwise stated:

Parameter	Interpretation	Value
β_i	Intrinsic birth rate of population *i*.	1 for i=1, 2.
c_1, c_2, c_3	Parameters of the cost-function	1, 9/20, 3/20
$c_{i,j}$	Scaling of the interactions	2 for $i = j$, 1 for $i \neq j$
$k_{i,j}$	Degree of asymmetry in the interaction	0 for all

Table 1. Parameter settings for the baseline scenario.

In figure 3 below, the axes represent the trait-values of the two populations, and the black lines are the zero-population size isoclines for the populations. We see that when $\Delta s = s_i - s_j$ is large, but both trait-values are close to the isoclines, they are determined by the cost-function, whereas when Δs is small (in the top right and lower left region) the interaction has an effect on the shape of the isoclines. Changing the values for β_i (equally for both populations) and the parameters in the cost-function will not affect the shape of the isoclines, only their positioning along the axis. Changing β_i for only one population, however, leads to a dramatic change in the region of coexistence, and for very different values ($\sim\beta_i > 3/2 * \beta_j$) the region seizes to exist. I do not explore this further and only minor changes in the β_i's are analyzed.

The region of coexistence is evidently independent of the degree of asymmetry in the interaction within a population as the degree of intraspecific asymmetry does not affect the impact of ecological competition ($\alpha(s_i, s_i, k_{i,i})$ is always ½). Changes in the inter-specific asymmetry, however, affect the isoclines in regions where Δs is fairly small. The only assumption we have made so far is that the interaction can be represented by the alpha-function defined, and that the traits are limited by the non-evolving environment (the δ-function). If we assume that competitive interactions follow this relationship in nature, then analyzing the size of the region of coexistence would relate to how often one would expect to encounter interactions with the specified parameters in nature. As one sees, the region is substantially smaller for large differences in β-values, which in turn means that competitive asymmetric interactions in nature may be more common between species with small or no difference in intrinsic birth-rates.

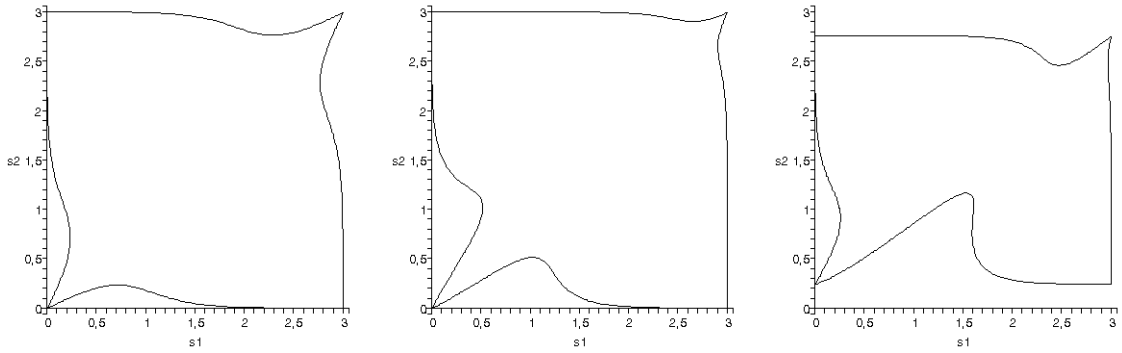

Figure 3. Regions of coexistence. a) Baseline scenario. b) Degree of inter-specific asymmetry, $k_{i,j}=3$. c) $k_{i,j}=3$ and $\beta_2=0.9$.

3.2 The fitness gradient.

One can get an impression of the dynamics of the model by inspecting the selection derivative. By differentiating the growth function of the mutant by the mutant trait-value, and then substituting it with the trait-value of the resident population in which it appears, one obtains;

$$\frac{\partial}{\partial s_{mut|i}} f_i\left(s_{mut|i}, s\right)\Big|_{s_{mut|i}=s_i} = \underbrace{\left(c_2 - 2\cdot c_3 \cdot s_i\right)}_{a} + \underbrace{\frac{2\cdot\gamma\cdot\hat{N}_j(s)\cdot c_{i,j}\cdot\left(s_i - s_j\right)\cdot\exp\left(-\left(s_i - s_j\right)^2\right)}{1+\exp\left(k_{i,j}\cdot\left(s_i - s_j\right)\right)}}_{b} + \underbrace{\frac{\gamma\cdot c_{i,j}\cdot\hat{N}_j(s)\cdot k_{i,j}\cdot\exp\left(k_{i,j}\cdot\left(s_i - s_j\right)\right)}{\left(1+\exp\left(k_{i,j}\left(s_i - s_j\right)\right)\right)^2}}_{c} + \underbrace{\frac{\gamma\cdot c_{i,i}\cdot\hat{N}_i(s)\cdot k_{i,i}}{4}}_{d} \quad \text{(XI)}$$

On first inspection one sees that the first term (*a*) is selection due to the cost-function defined. This term will always point towards the optimum trait-value, only augmented by the other terms (*b*-*d*) which result from the ecological interaction within and between the populations. If there is only one populations, (i.e. N_j =0) then the only other term is the last (*d*), which will be positive for all positive values of $k_{i,i}$ (the degree of asymmetry within population *i*). This makes intuitive sense, since an increased level of asymmetry within a population should lead to an equilibrium trait-value higher than the optimum defined by the cost-function. Note that *d* is here *not explicitly* dependent on the trait-value of the population in focus. However, the equilibrium population sizes in this equation are in themselves dependent on the trait-values, which make the fitness gradient highly nonlinear. Note also that γ always appears together with the equilibrium population sizes, and therefore γ does not affect the dynamics directly, although it will affect the *speed* of the dynamical system by scaling the population-sizes which appear in the kappa-function in the canonical equation (here the γ's will be cancelled out, see equation X).

The *b* and *c* terms in equation XI are the results of the ecological competition between the populations, and therefore depend on the trait-values of both populations, the population size of the competitor, and the different parameters scaling the interaction. The *c* term is always positive (or zero), whereas the *b* term depends on the difference in trait-values and may therefore take both positive and negative values. One can see that *b* will be negative for the population with the smaller trait-value and positive for the larger, and

thus lead to selection towards smaller trait-value for the former and opposite for the larger. One also sees that the *c* term is directly dependent on the level of asymmetry in the inter-specific interaction, and therefore is zero in the case of symmetric competition.

To have selection for smaller (larger) trait-values arising from the interspecific interaction, the sum of the second and the third term needs to be negative (positive) (note though that there is a possible negative term arising from the cost-function). Some algebra gives rise to the following necessary condition for selection for smaller trait values to occur due to the inter-specific competition:

$$2 \cdot \Delta s + \frac{k_{i,j} \cdot \exp\left(k_{i,j} \cdot \Delta s\right)}{1 + \exp\left(k_{i,j} \cdot \Delta s\right)} < 0 \qquad \text{(XII)}$$

We see immediately that when there is no asymmetry in the interaction, the inequality only holds for negative differences in trait values, i.e. always for the population with the smaller trait-value. When there is asymmetric competition it will still only hold for negative Δs but not necessarily all. With increasing levels of asymmetry one sees that there are possible negative differences in trait values for which the interaction will lead to selection for larger trait-values. When this is the case the population with the smaller trait-value will experience selection for larger trait size arising from the asymmetric interaction with the competitor with the larger trait value. This is a result of Δs not being large enough in absolute terms for the two populations to be on different sides of the peak in the α-function (see figure 1). If the populations are similar (Δs is small) increasing levels of asymmetry may lead to larger mutants being favored in both populations and can only be augmented by the cost of increasing trait-values. Limit cycles in the model will probably include evolution within and outside this range, at least for one of the populations.

Inequality XI also reveals that the species with the larger trait value will only experience selection for smaller trait-values arising from the cost-function and never from the interactions within or between the populations. Thus the only cases in which the model may exhibit cycles are when selection due to the ecological interaction becomes weaker (in absolute terms) than selection for optimum trait-value for the larger population. This

implies that a decrease in the trait-value of the species with the smaller trait value has to predate a decline in the other species.

The null-isoclines for the fitness gradients of both populations are of particular interest with respect to the evolutionary dynamics. These isoclines describe where the selection derivative equals zero, and therefore where adaptive evolution in one of the populations stops. Depending on the system, the realization of the solutions will either tend to or from the isoclines. Where the evolutionary isoclines of the two populations intersect, we have an evolutionary singular point (Geritz et al. 1998). These evolutionary singular points represent possible evolutionary outcomes, depending on the shape of the isoclines. When I numerically solved the dynamical system defined by XI and VI, I incorporated the unique non-zero solutions to the population dynamics so that the evolution of the system only depends on the trait-values. The isoclines in the model presented here were to complex to be solved analytically. Accordingly, I relied on numerical analysis using Maple (Maplesoft. 2003)

3.3 Properties of evolutionary singular strategies.

Recall the properties used to characterize the dynamics around a singular strategy (or a coalition of two strategies) (Geritz et al. 1998):

$$\text{(a)}\ \frac{\partial^2}{\partial s_i^{\,2}} f\left(s_{mut|i}, s\right)\Big|_{s_{mut|i}=s_i} \qquad \text{(b)}\ \frac{\partial^2}{\partial s_{mut|i}^{\,2}} f\left(s_{mut|i}, s\right)\Big|_{s_{mut|i}=s_i}$$

For the model presented here the properties are;

$$\frac{\partial^2}{\partial s_i^{\,2}} f\left(s_{mut|i}, s\right)\Big|_{s_{mut|i}=s_i} = \gamma \cdot c_{i,i} \cdot \left(N_i\left(s_1, s_2\right) - \frac{1}{2} \cdot k_{i,i} \cdot \left(\frac{\partial}{\partial s_i} N_i\left(s_1, s_2\right) \right) - \frac{1}{2} \cdot \left(\frac{\partial^2}{\partial s_i^{\,2}} N_i\left(s_1, s_2\right) \right) \right) - c_{i,j} \cdot \alpha\left(s_i, s_j, k_{i,j}\right) \cdot \left(\left(\frac{\partial^2}{\partial s_i^{\,2}} N_j\left(s_1, s_2\right) \right) \right) \quad \text{(XIII, a)}$$

$$\frac{\partial^2}{\partial s_{mut|i}^{\,2}} f\left(s_{mut|i}, s\right)\Big|_{s_{mut|i}=s_i} = -2 \cdot c_3 + \gamma \cdot c_{i,j} \cdot N_i + \left(c_{i,j} \cdot \alpha\left(s_i, s_j, k_{i,j}\right) \cdot N_j \cdot \left(2 - 4 \cdot ds^2 + \frac{k_{i,j} \cdot \exp\left(k_{i,j} \cdot ds\right)}{1 + \exp\left(k_{i,j} \cdot ds\right)} \left(k_{i,j} - 4 \cdot ds - \frac{2 \cdot k_{i,j} \cdot \exp\left(k_{i,j} \cdot ds\right)}{1 + \exp\left(k_{i,j} \cdot ds\right)} \right) \right) \right) \quad \text{(XIII, b)}$$

These expressions are fairly complex, but numerical exploration of term *a*, shows that it is usually positive in the region of coexistence, and almost always so in the regions where

we experience an equilibrium point. There is also valuable insight to be gained from applying the conditions for evolutionary branching to occur. These conditions are again ($b > 0$, $a - b > 0$, and $a + b > 0$). One parameter of particular importance (even though the rest of the expression will be complex) here is $c_{3,}$ the last parameter in the δ-function. If this parameter has a low numerical value (remember it is assumed to always be positive) it can increase the probability that two of the conditions for branching to occur are fulfilled. This makes sense when we recall that the last parameter in the δ-function defines the steepness of the function, i.e. how narrow the regions of viable trait-values are. When c_3 has a low value, there is a wider scope of possible trait-values in which coexistence is attainable (a wider range of unutilized resources), and therefore the possibility for evolutionary branching caused by the ecological interactions in the model is increased. Since this only applies in the vicinity of a convergence stable equilibrium, c_3 can be interpreted as defining the steepness of the distribution of resources surrounding the singular point. Note, however, that a lower value for c_3 may also lead to larger differences in trait-values, which also influence b. Hence, the relationship between c_3 and the possibility for evolutionary branching is complex.

3.4 Conditions/criteria for limit cycles.

It is hard to identify or analytically show the existence of limit cycles in a dynamical system. To evaluate whether cycles may occur in the system I applied and numerically investigated the Bendixson-Dulac theorem (e.g. Farkas (1994)) also called Dulac's criterion. The theorem states;

Given $\dot{z} = f(z)$, $z \in R^2$ and $div(f) = \frac{\partial f_1}{\partial z_1} + \frac{\partial f_2}{\partial z_2}$

If $div(f) \neq 0$ almost anywhere in the region of interest then the plane autonomous system does not have any periodic solutions. "Almost anywhere" here means everywhere except for a point or a line, i.e. a set with area 0.

These conditions were implemented and tested numerically for all parameter settings used in the investigation. Interestingly, $div(f)$ was always equal to zero in some parts of

the plane. When the theorem failed to yield any results, I resorted to investigate the model numerically, to localize the equilibria of the set and to investigate the eigenvalues of the Jacobian at the equilibria. The existence of limit cycles cannot be ascertained by only inspecting the Jacobian, however, so I also used numerical simulations of the equations.

3.5 Evolutionary dynamics.

3.5.1 Baseline scenario.

As for the investigation of the regions of coexistence, a baseline scenario for the evolutionary dynamical model is presented, with parameters as shown in table 2.

Parameter	Interpretation	Value
μ_i	Mutation rate	10^-4
σ_i^2	Mutational variance	10^-3
γ	Scaling of population sizes	1/500

Table 2. Parameter settings for the baseline scenario.

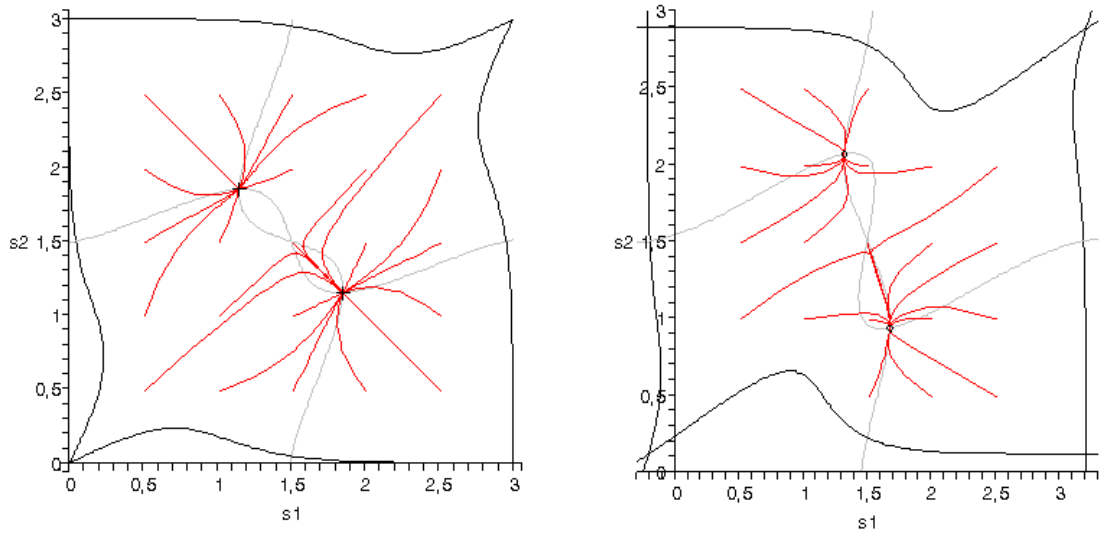

Figure 4. Phase portrait of evolutionary baseline-scenario. Isoclines for non-negative population sizes in black, evolutionary isoclines in grey. Crosses mark attractors with strong convergence stability , but not ESS stability for any, diamonds indicate attractors with strong convergence stability and ESS stability only for population 2. Parameter values in a: $\beta_1 = \beta_2 = 1$, and in b: $\beta_1 = 22/20$, $\beta_2 = 19/20$.

Figure 4 shows both the zero-population size isoclines (black) and the evolutionary isoclines (grey) of the baseline scenario and a scenario with differing β-values in addition to several numerical simulations of the systems (red). As is apparent in 4a), the evolutionary isoclines intersect in three points, one saddle (s_1=s_2=1.5) and two attractors that are equivalent, in the sense that their trait-values are opposite. It is not shown in the figure, but inspecting the numerical simulations suggest that the saddle's unstable manifolds flow towards the attractors and its stable manifolds attract towards the saddle from the saddles where the isoclines for zero-population size intersect in [0,0] and [3,3]. For the values stated in table 1, the attractors are not ESS stable ((b)>0), and therefore constitutes branching-points. This has been explored thoroughly in earlier models of asymmetric competition (Kisdi 1999), and will not be explored further. Using a higher value for c_3 will in the baseline scenario only lead to one monomorphic equilibrium, which is both ESS and convergence stable for both populations.

The evolutionary orbits depend on the initial conditions. We can recognize both parallel shifts (both populations increase or decrease in trait-value) and divergence after some time. The coevolutionary path undertaken can also entail reversal of the direction of evolution in one population, as the other evolves to larger trait size. This is particularly evident where the initial trait sizes are fairly equal and different from the optimal size. In these simulations selection on both populations is firstly determined by the environment (i.e. δ- function) but as they evolve closer to the optimum, they diverge due the competitive interaction.

In figure 4b the birth rates are different for the two populations. The resulting evolutionary attractors are convergence stable for both populations, but ESS stable only for population 2. They constitute branching points for population 1. The rationale for this is that $\beta_1 > \beta_2$. Accordingly, population 1 has a larger range of resources to consume and has therefore a higher potential for branching into 'unused' resource-space, whereas this is not the case for population 2.

3.5.2 Asymmetric intraspecific competition.

To investigate the model I varied the parameters of interests individually and in concert. Intra and interspecific asymmetries in the competitive are not necessarily correlated. One can for instance easily imagine species where there is contest-like competition within the species (which is of a more asymmetric nature), say for territories, while the inter-specific competition is more based on resource utilization and not associated with such contests. The simplest scenarios of asymmetric intraspecific competition are presented in figure 5. Except for the values stated in the figure(s) all are set as in table 1 and 2.

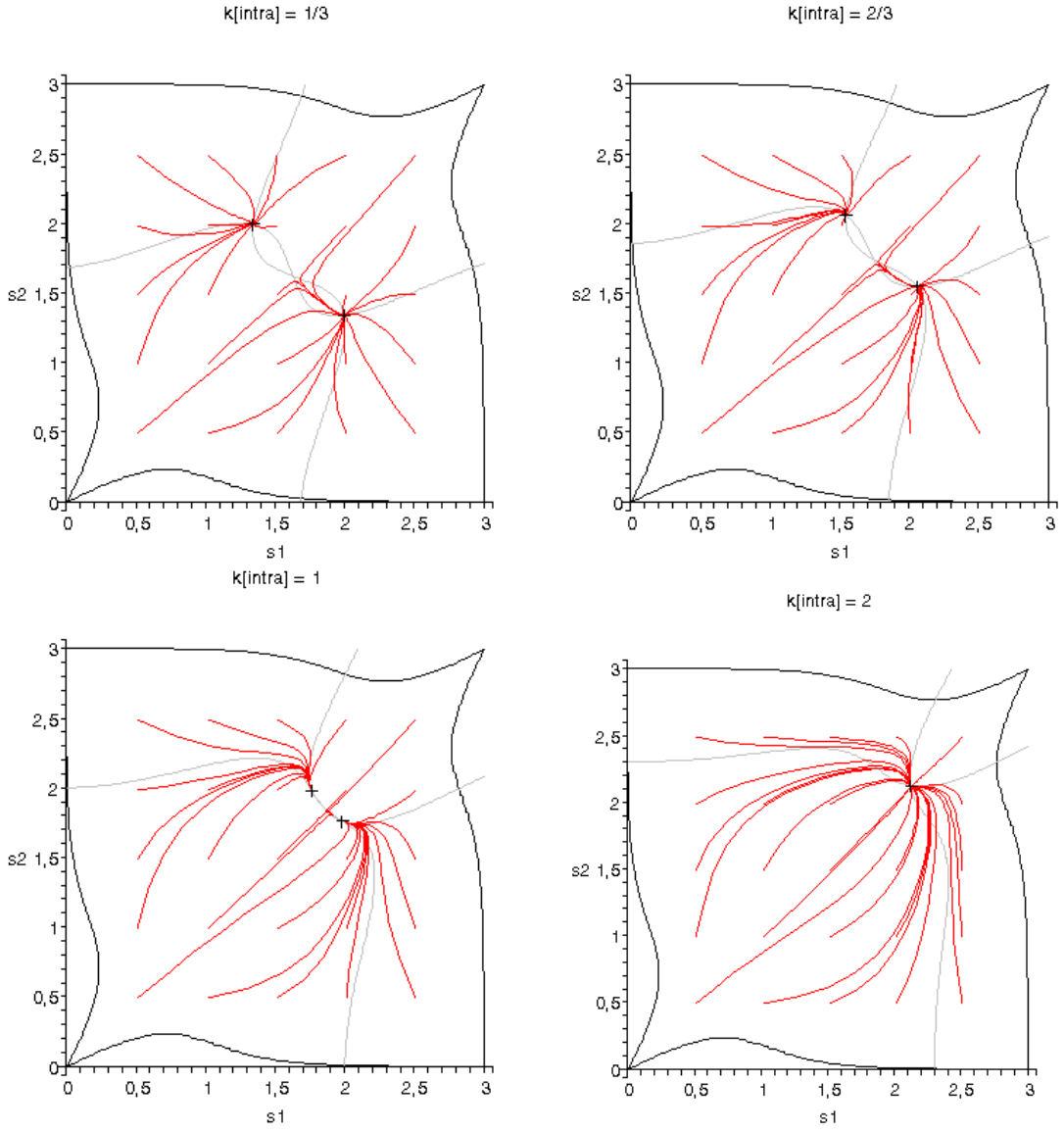

Figure 5. Phase-portraits for different values of the intraspecific asymmetry parameter, $k[intra]=k_{i,j}$, $i \neq j$.

What is apparent and also expected is that the convergence stable resting points increase in value as the degree of asymmetric intraspecific competition increase. We also see that the system undergoes a pitchfork bifurcation where $k_{i,i}$ exceeds 1. The only stop for evolution of this system (figure 5d) is an evolutionary attractor which is not ESS stable for any of the populations. The degree of asymmetry selects for larger and larger traits, and leaves a large part of the resource space unutilized, the populations with $k_{i,i}=2$ both converge to a monomorphic equilibrium with fairly large trait sizes. A single population model with the same settings also yielded an evolutionary branching point at that trait-value, and an extension of this (i.e. $c_{i,i}=c_{i,j}$) yielded a polymorphic equilibria ESS stable for the larger species (results not shown).

3.5.3 Asymmetric interspecific competition.

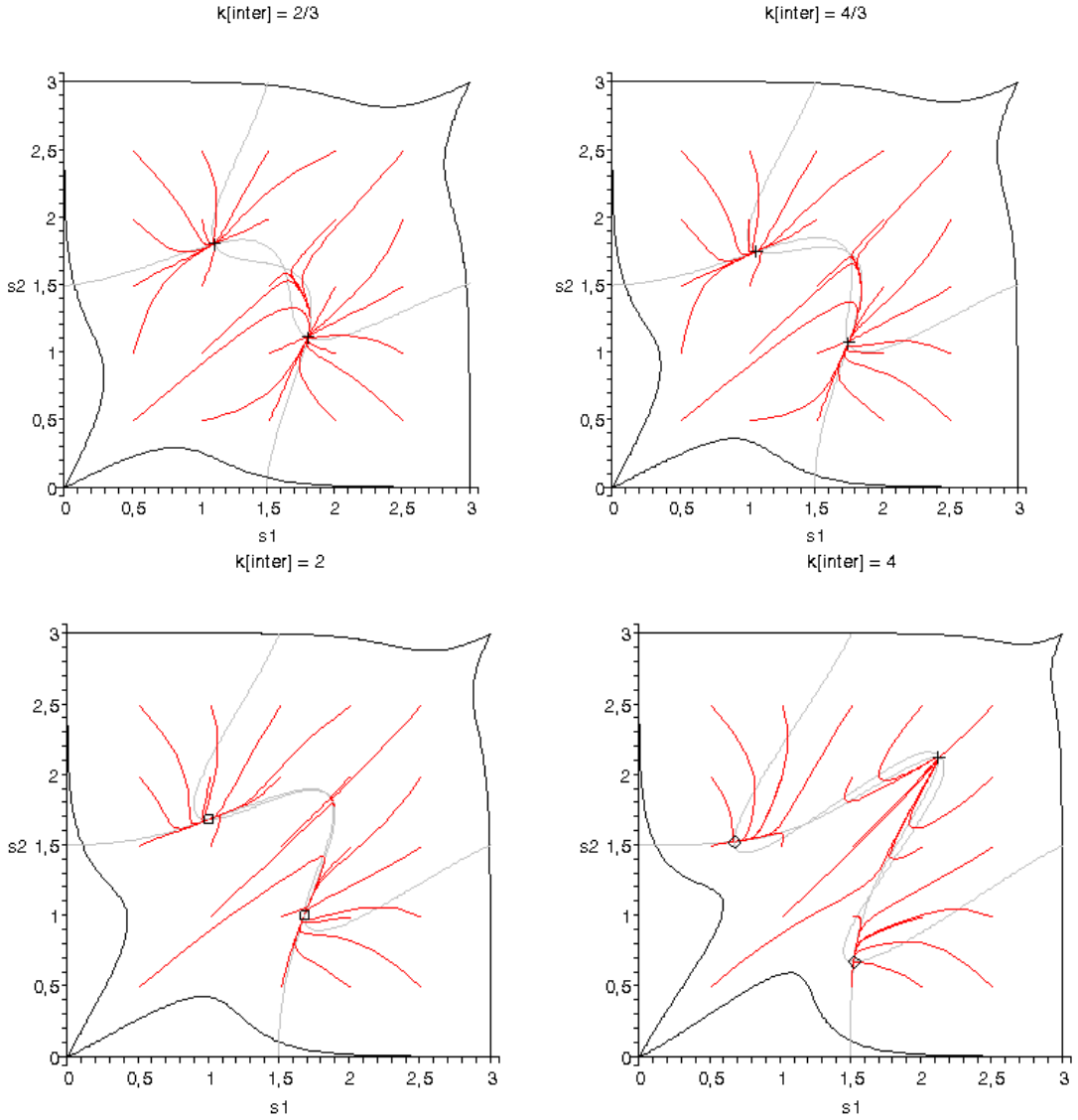

Figure 6. Phase-portraits for different values of the interspecific asymmetry parameter. Only equilibria which are dynamical attractors are depicted with points, crosses are attractors that are not ESS stable for any population, diamonds are ESS-stable for one population and boxes are not ESS stable for any and convergence stable for only one of the populations.

In figure 6 the effect of different asymmetries in interspecific competition is illustrated. What is interesting to see is that the evolutionary isoclines shift in a qualitatively different manner compared to the scenarios where I varied the intraspecific degree of asymmetry (figure 5). In case of intraspecific asymmetries the isoclines shifted more in position than

in shape, but in case of interspecific asymmetries (figure 6) one sees that they change shape within the region of coexistence.

3.5.4 Asymmetric inter- and intra-specific competition.

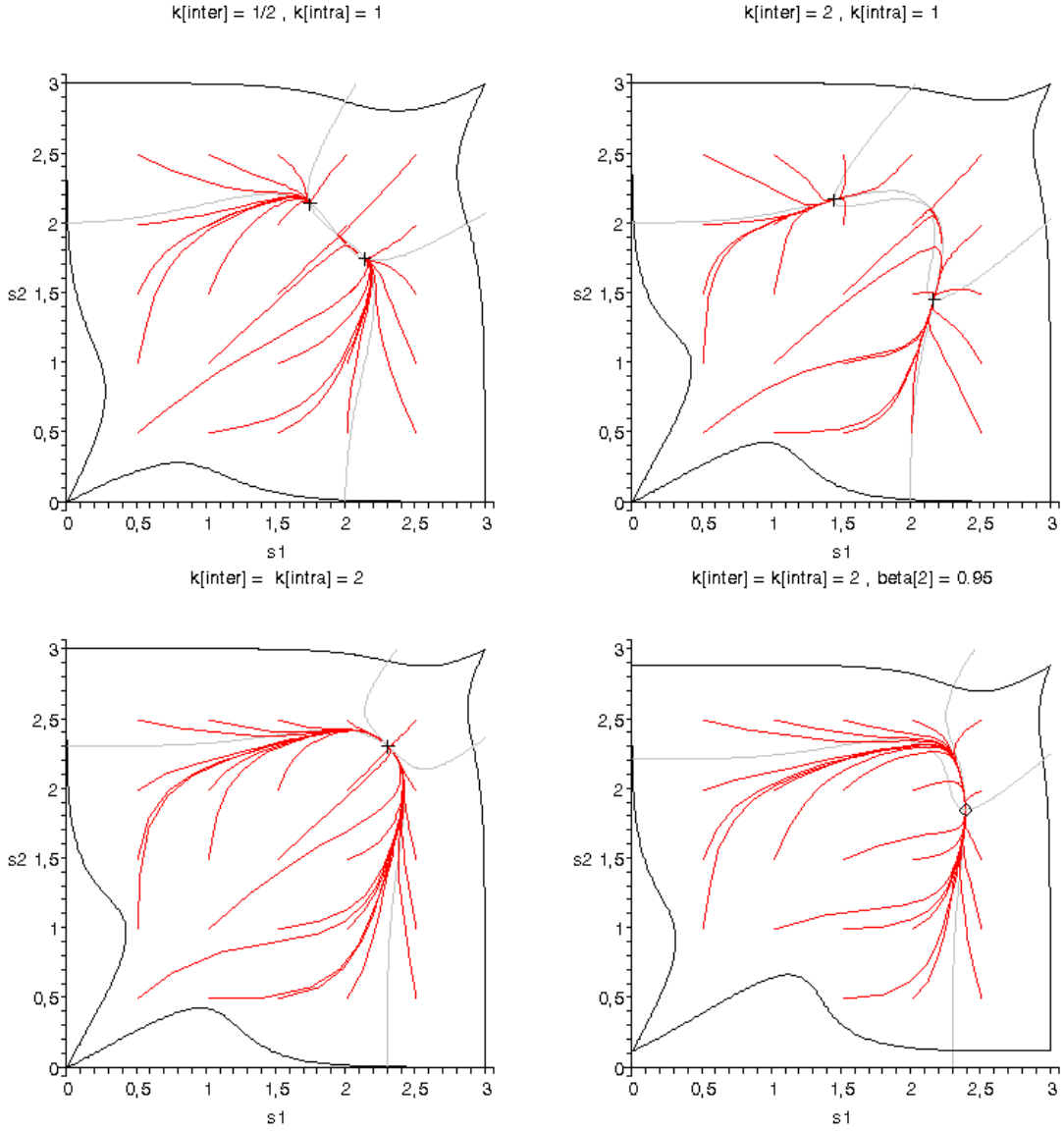

Figure 7. Phase-portraits for different values of inter- and intra-specific asymmetric interactions.

Figure 7 displays the evolutionary dynamics for various settings of both inter- and intra-specific asymmetric competition. As also seen in the previous sections, the degree of intra-specific asymmetry mainly changes the positioning of the evolutionary isoclines, whereas the degree of inter-specific asymmetry mainly changes the shape more than the positioning. The changes in shape are however less pronounced with a higher degree of intraspecific asymmetry. This can be interpreted in the sense that it is the intra-specific

interaction that predominantly defines the evolutionary dynamics here, probably due to the different impacts of between and within interactions.

3.5.5 Red Queen dynamics.

3.5.5.1 Limit cycles in the deterministic model.

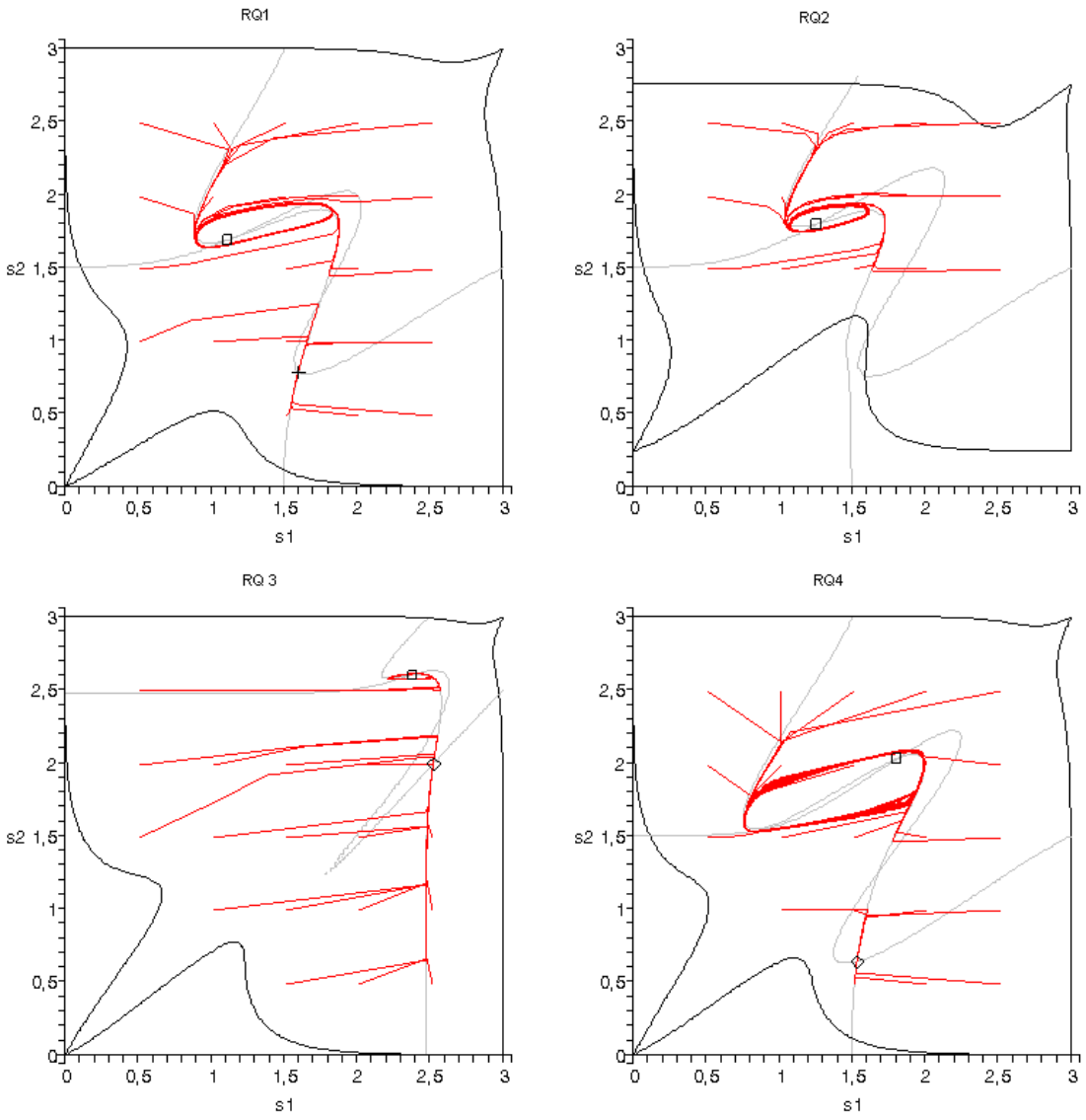

Figure 8: The Red Queen dynamics of scenario 1 through 4. For parameter setting see table 3.

Parameter	Scenario RQ1	Scenario RQ2	Scenario RQ3	Scenario RQ4
β_1 , β_2	1, 1	1, 0.9	1, 1	1, 1
$c_{i,i}$, $c_{i,j}$	2 , 1	2 , 1	2, 1	2, 1
c_1 , c_2 , c_3	1, 9/20 , 3/20	1 , 9/20 , 3/20	1 , 9/20 , 3/20	1 , 9/20 , 3/20
$k_{1,1}$, $k_{1,2}$, $k_{2,1}$, $k_{2,2}$	0 , 2 , 3 , 0	0 , 3 , 3 , 0	3 , 5 , 7 , 3	0 , 3 , 5 , 0
γ	1/500	1/500	1/500	1/500
σ_1^2 / σ_2^2	1	1	1	1
μ_1 / μ_2	10	7	40	10

Table 3. Parameter settings for Red Queen dynamics scenarios.

In figure 8 four examples of scenarios with evolutionary cycling is depicted for different parameter-settings. They all entail a certain degree of asymmetry in the inter-specific competitive interactions and different evolutionary rates for the two populations. The population with the faster evolutionary rate always has the higher amplitude in the cyclic trait. One interesting feature of scenario RQ4 is that the two populations alternate in having the largest trait-value, i.e. at some point in the cycle the larger becomes the smaller and vice-versa. To my knowledge this result has not been reported before as a potential result of competitive interactions.

The different parts of the selection derivative for scenario RQ2 is depicted for the two populations in figure 9. What is interesting is that population 2 (with the largest trait size but smallest amplitude of the cycle) always experiences selection for larger trait size due to the interaction and for smaller trait size due to the δ-function, while population 1 experiences both positive and negative selection due to both. This is also evident in figure 10, where inequality XII is shown for both populations in scenario RQ2.

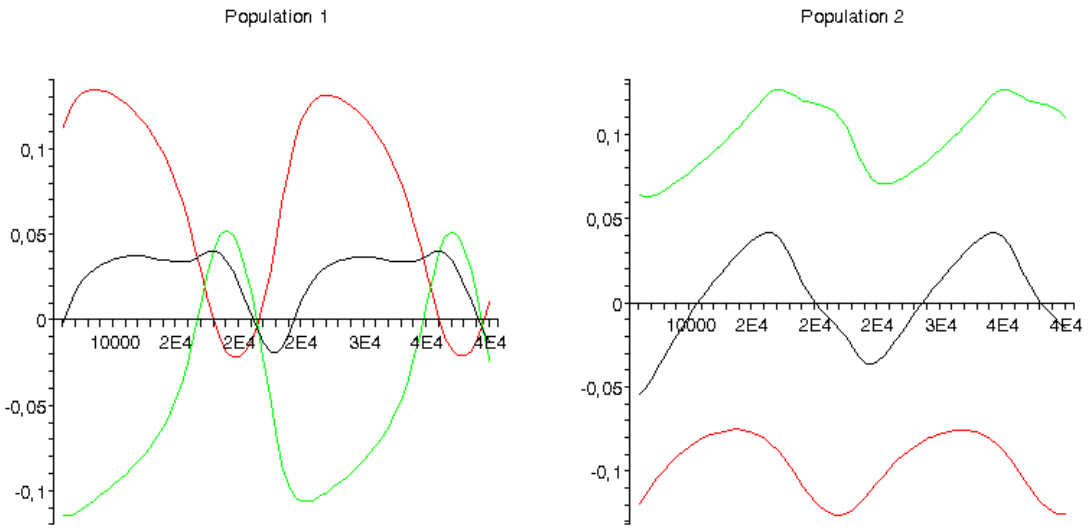

Figure 9. Partitioning of the different parts of the selection derivative for the two populations at the limit-cycle attractor in RQ2. Green lines illustrate the parts b and c (d is non-existent due to no intraspecific asymmetry) of equation X (selection due to the ecological interaction), red the selection toward the optimum trait-value and black lines the total, i.e. the direction of evolution in the population.

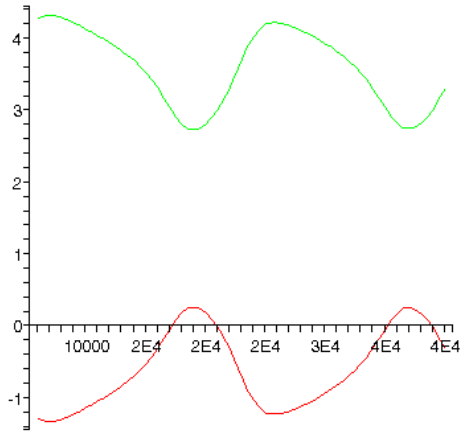

Figure 10. Displays the value for left hand side of inequality XII. Red is population 1 and green population 2. What is easily seen is that only population 1 undergoes both selection for larger and smaller trait-values due to the ecological interaction.

Thus the continual evolution is driven by fast trait evolution in population 1 that 'pushes' population 2 towards the end of the resource spectrum, while population 1 itself is not that adversely affected due to a higher β-value. Population 1 actually undergoes evolution

such that it comes close enough in trait-value to population 2 that it experiences positive selection due to the interspecific interaction (see figure 10). All cycles found in the model consist of one population being 'squeezed' between selection arising from the interaction and that from adapting to the environment, and it is always the faster evolving population that is the 'pusher' and the slower that is being pushed. This also relates to the equilibrium population sizes of the two populations as they undergo a cycle, as these sizes change and thereby affects the selection derivative.

The cycles are very sensitive to changes of the parameters in the δ-function as seen in figure 11, where c_3 is varied around the baseline value of 6/40 for scenario RQ2. One sees that the system undergoes a bifurcation as c_3 is changed from 5/40 towards 6/40 and that the system undergoes another bifurcation as c_3 is changed from 6/40 towards 7/40. This change of parameters would constitute environmental forcing, e.g. by change of climate, such that the resources consumed by the populations change in distribution and abundance.

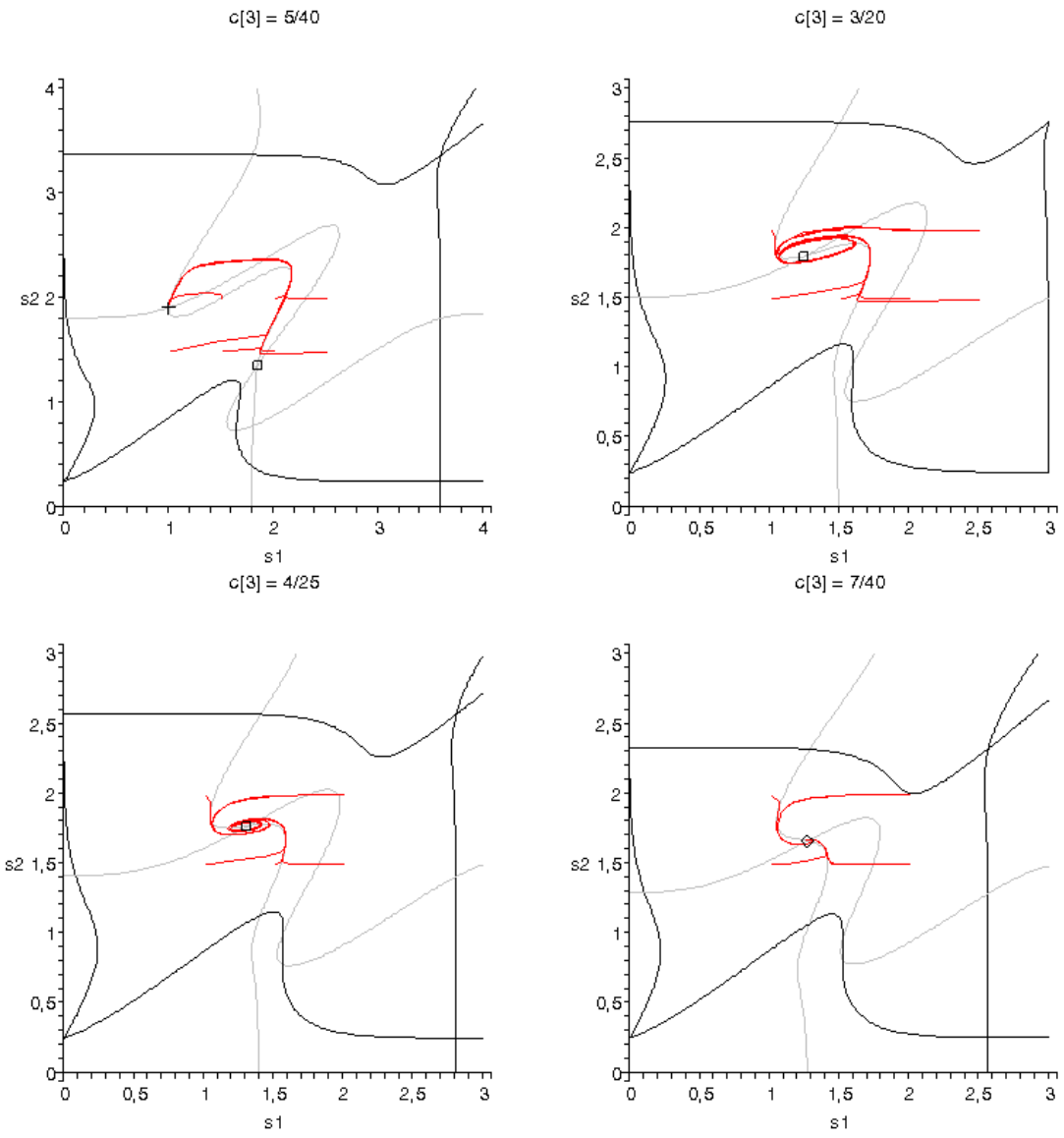

Figure 11. Parameters as in the scenario with only interspecific asymmetry (RQ2). The c_3 values are indicated on each figure. Note the different scale in a vs. b-d.

3.5.5.2 Limit cycles in the monomorphic stochastic model.

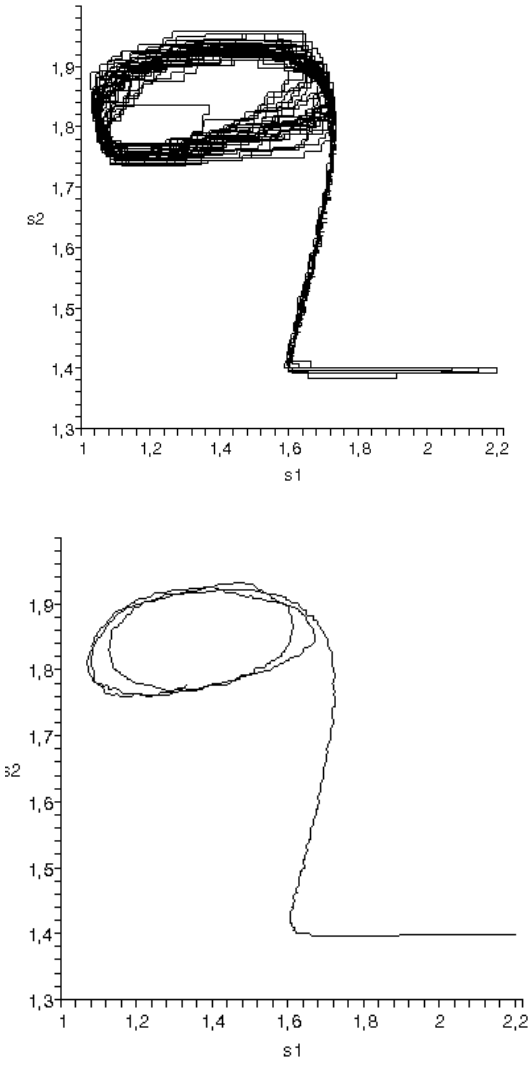

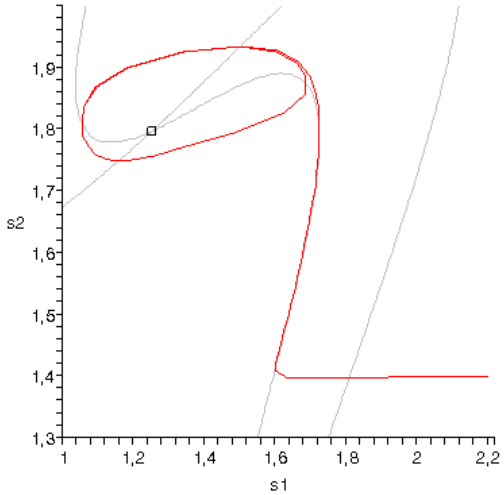

Figure 12. Realizations of the monomorphic stochastic model, with parameter-settings as in scenario RQ2. Top left shows eight simulations with same initial values, and bottom left shows the average of the simulations. Above is the deterministic approximation where the evolutionary isoclines are also depicted.

The monomorphic stochastic model represents each population with one trait-value and calculates transitional probabilities to other trait-values in the vicinity according to the invasion-fitness and mutational distributions. In figure 13 I have depicted several simulation runs with the model for scenario RQ2. The cycle predicted by the deterministic approximation is evident, with stochastic variations around the mean. Every run is somewhat different due to the stochasticity, but the mean is not very different from the differential equation approximation.

3.5.5.3 Limit cycles in the polymorphic stochastic model.

One reassuring aspect of the existence of limit cycles is that they easily appear in both the deterministic approximation and the monomorphic stochastic model. On the other hand, how the evolutionary trajectories will display in an individual-based stochastic model will probably largely be determined by the amount of phenotypic variance included in the model populations. This variance in trait-values can be manipulated by altering the values for mutation rate and mutational variance, but also by the scaling the population sizes (in this model the value of gamma, see appendix 2), because larger population sizes leads to lower probability for any particular individual to die (in essence larger populations scales all the probabilities down so that the fitness difference between individuals becomes less pronounced).

In figure 13 (below) one sees that the limit cycle attractor is also emergent in the individual-based simulations (the scenario is the equivalent of RQ2, but the simulation was run with different values for the delta-function due to later adjustment of those parameters to fit the region of coexistence into the positive quadrant). As the parameter-settings in the scenario imply, with differing mutation rates, population 1 exhibits more variation around the predominating trait-value. And as predicted by the deterministic approximations, the amplitude of the cycle is much larger for population 1 (note the difference in scales on the y-axes). Simulations where one of the populations went extinct due to the stochasticity were frequent, even though the solution for the population sizes (XI) were positive. Several simulation runs were conducted before a value of γ=1/500 was chosen in all models, which lead to a decrease in extinctions.

For the evolving populations to follow the orbit predicted by the deterministic model, the variance has to be small in comparison with the amplitude in trait-values the cycle will exhibit.

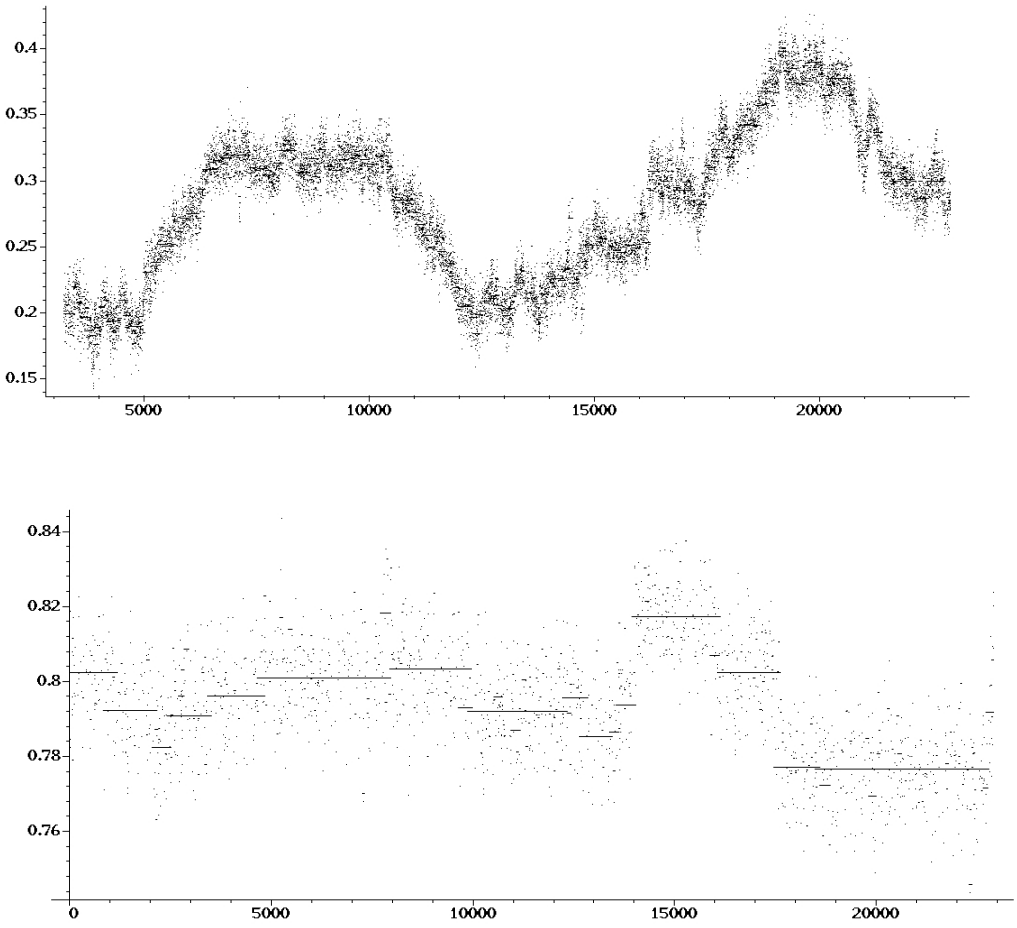

Figure 13. Realization of the individual-based model with values for the limit cycle presented in scenario 2, except for the parameter in the cost-function, here $c_1=5/10, c_2=3/10, c_3=3/10$. Top, population 1, bottom; 2. Note the different y-axes.

3.6 The importance of evolutionary rates.

The limit cycles identified in the model can be shown to occur through Hopf-bifurcations, where a stable focus bifurcates into an unstable focus with a surrounding limit cycle. The eigenvalues of the Jacobian at an equilibrium reveal the nature of these equilibria and the occurrence of a Hopf-bifurcation. As shown in appendix 3 all cycles found occur through Hopf-bifurcations when one varies the evolutionary rate (i.e. the κ-function) of one of the populations when the equilibria is convergence stable for only one of the coevolving populations.

Convergence stability is an independent measure of local asymptotic stability of the dynamical system, and one can linearize the dynamics around an equilibrium with the Jacobian of the system;

$$\mathbf{J} = \left[\begin{array}{cc} \kappa_1(s)\left(\frac{\partial^2 f_1(s_{mut|1},\mathbf{s})}{\partial s_1 \partial s_{mut|1}} + \frac{\partial^2 f_1(s_{mut|1},\mathbf{s})}{\partial s_{mut|1}^{\,2}} \right) & \kappa_1(s)\left(\frac{\partial^2 f_1(s_{mut|1},\mathbf{s})}{\partial s_{mut|1} \partial s_2} \right) \\ \kappa_2(s)\left(\frac{\partial^2 f_2(s_{mut|2},\mathbf{s})}{\partial s_{mut|2} \partial s_1} \right) & \kappa_2(s)\left(\frac{\partial^2 f_2(s_{mut|2},\mathbf{s})}{\partial s_2 \partial s_{mut|2}} + \frac{\partial^2 f_2(s_{mut|2},\mathbf{s})}{\partial s_{mut|2}^{\,2}} \right) \end{array} \right]_{s_{mut}=s=\hat{s}}$$

The elements on the diagonal correspond to the criteria for convergence stability for each population, and in the case of convergence stability for only one population, these are of different signs. As noted by Marrow and Dieckmann (1996); in scenarios where this is the case, different dynamics can be achieved around the fixed point. This was further elaborated by Leimar (2002), where the investigation of the mutational matrix (which in this case would be a diagonal matrix $\boldsymbol{A}$ where $\boldsymbol{A_{i,i}=\kappa_i}$) was suggested as a method to determine the stability of the point. Given convergence stability for only one population, if the off-diagonal elements in the Jacobian above are of same sign, the point is an attractor, but if they are of opposite signs the stability depends on the κ-functions. This change of stability as one varies a parameter in the κ-functions corresponds to a Hopf-bifurcation. The derivation for the bifurcation is described in detail in appendix 3.

The Hopf-bifurcation is a local bifurcation, and it will occur as described above if the conditions are satisfied. Over how large part of the parameter-space the limit cycle will

continue to exist depends on the global phase-portrait. The linearization (i.e. the Jacobian) around an equilibrium can show the transition from a spiral sink to a spiral source, but it is only in the infinitesimal vicinity of the bifurcation-point that we can be sure about the existence of a cycle. It can in many cases be a transient phenomenon, and the destiny of a limit cycle depends on the global phase-portrait as it turns into a source and acts as a repellor. If one inspects the evolutionary cycle in scenario RQ3 the limit cycle has a very small amplitude and does not exist in a large parameter subspace.

Figure 14 depicts the evolutionary dynamics of the limit cycle RQ4 as one varies the parameters in the κ-function for one of the populations. Here $\rho = \mu_1 / \mu_2$. We can see that the system undergoes a Hopf-bifurcation as one varies the mutational rates. The exact bifurcation ($\rho \approx 100/17.6$) was calculated and predicted using the insight in appendix 3.

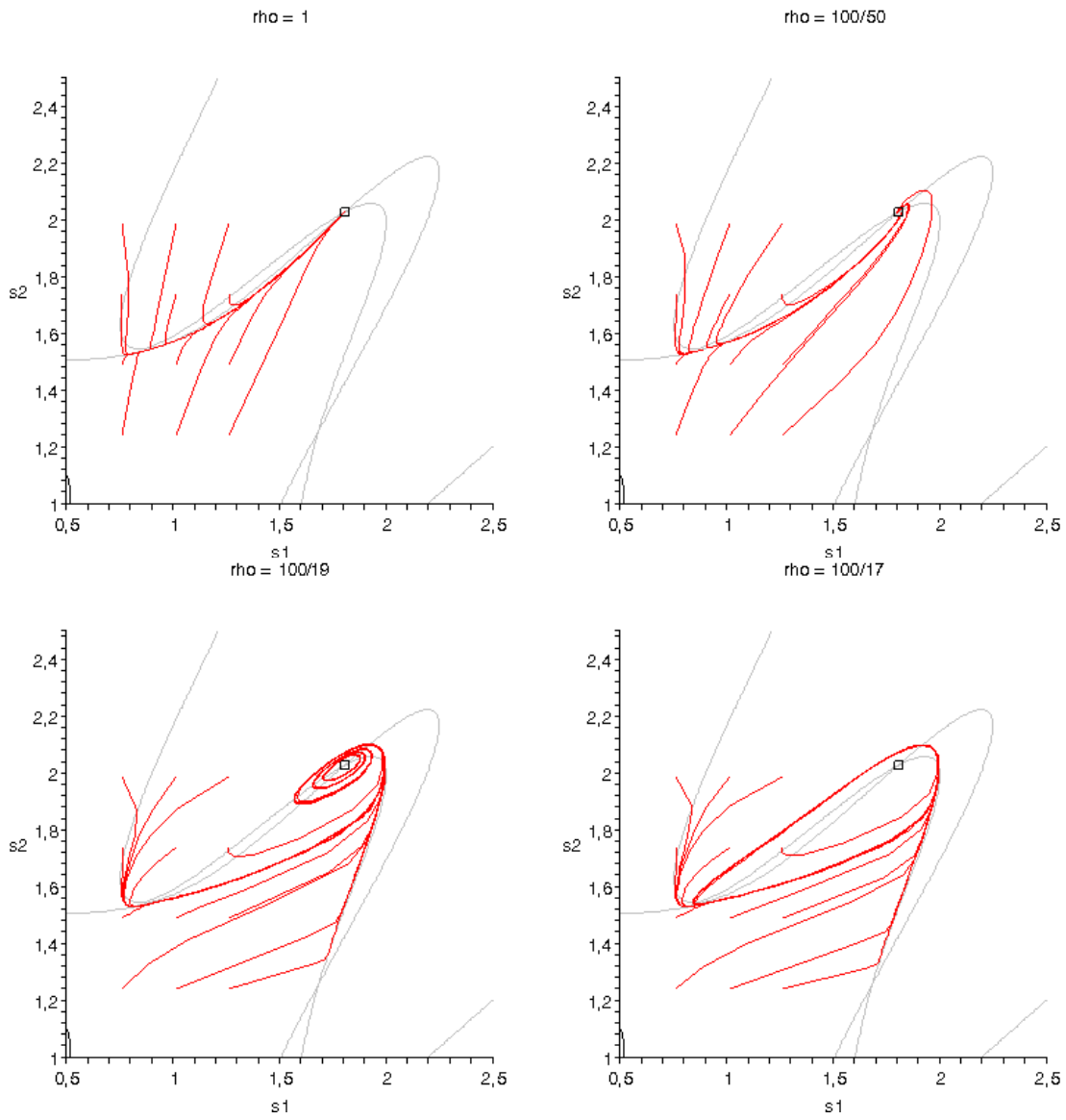

Figure 14. The Hopf-bifurcation in RQ4. All parameters are as in table 3, except for μ_1 and μ_2 which are scaled such that $\rho=\mu_1/\mu_2$.

It is important to understand that the above scenario is not the only way to achieve limit cycles in a dynamical system like the one presented here. This is but one way the eigenvalues of the Jacobian can characterize a Hopf-bifurcation, and non-stationary dynamics can also occur through other bifurcations and in different guises (e.g. a homoclinic loop). But to draw similar conclusions for the other parameters are more problematic, because they do not only alter the dynamics exhibited, but also the positioning of the equilibria (see figure 11. for changes in c_3). In addition, the partial

derivatives may change dramatically. However one can follow these bifurcation points through numerical continuation and probably reveal parts of the parameter-space where the two populations have the same parameters in $\kappa(s)$, but still show limit cycles.

The localization of parameter-settings that yield limit-cycles becomes easier when one realizes the above relationships, and I found several more limit-cycle attractors, using the procedure of scaling the ratio of evolutionary rates after localizing an attractor with the above conditions.

4. Discussion

4.1 On evolution under asymmetric competition.

The dynamics of the co-evolutionary system presented were heavily influenced by the degree of asymmetry in the competitive interactions. An increasing level of intra-specific asymmetry leads to evolution toward larger trait sizes of the population, as we saw a shift in the positioning of the evolutionary isoclines. It also increased the likelihood of both populations to converge to the same trait size, though these attractors were rarely ESS stable. Inter-specific asymmetry had a highly nonlinear effect, changing the shapes of the isoclines and affecting the dynamics in a qualitatively different manner than intra-specific asymmetry, and could increase the number of attainable equilibria. In scenarios of asymmetry in both intra- and inter-specific competition, the level of asymmetry within a population had the dominating effect on the dynamics. Only when the evolutionary rates of the populations were different, and there was asymmetric competition between the populations did the model yield non-stationary Red Queen dynamics in the form of limit cycles.

What is interesting is the fact that the model presented predicts a larger region of co-existence with higher degree of asymmetry, whereas the model by Law et al.(1997) predicts there to be a smaller region. This is most likely due to the way they define the competitive interaction, where a large difference in trait-values yields as much impact as a smaller difference (see figure 1). In my model the competitive interactions only have an effect on the zero population isoclines when Δs is small. Law et al. (1997) also highlighted the importance of directly (numerically) investigating adaptive dynamics models, due the lack of analytical conditions showing the existence of periodic orbits of evolution. As they state: 'There appears to be no shortcut…' (Law et al. 1997). I indeed found and presented one shortcut for finding such periodic orbits, given that one can locate an equilibrium with the conditions described in appendix 3. This is also one way to obtains the limit cycle presented in their paper. As this is achieved through changing the parameters in the κ-function, the conditions apply to any two-dimensional dynamical system with such scaling-factors, and therefore any adaptive dynamics co-evolutionary

system of two populations. That some equilibria which are convergence stable for only one population can change dynamical stability through such scaling was however briefly mentioned in Marrow et al. (1996) and elaborated somewhat by Leimar (2002), though they seemed to have missed the fact that the system can be forced through a Hopf-bifurcation.

The appearance of branching-points in the model presented is predominant. It is therefore important to appreciate that the construction of the model was with focus on co-evolution, and that the dynamics of the model is not an extension of a one-species model in which there occurs evolutionary branching. This is solely due to the scaling of the interactions to be of different impacts between and within populations, i.e. different values for $c_{i,i}$ and $c_{i,j}$. As an example, a one population model with parameters as in the baseline scenario would predict there to be a branching point at $s_1 = 1.5$, but the model presented here would not constitute an extension of such a model, because here we scale the interaction differently between the populations. Kisdi's (1999) investigation of circumstances in which asymmetric competition would lead to evolutionary branching showed that branching is commonly the case. She did not assume any particular shape of the equivalents of the α – and δ-functions used here, but instead used their shapes characterized by the second derivatives. According to her analysis, functions as defined here can give rise to both continuously stable strategies/coalitions (CSS's after Eshel (1983)) or branching points. Even though this analysis only applies to one-population systems, both convergence stable, ESS stable coalitions, and branching points were found in my model. Kisdi's (1999) classification did not include any analysis of potential for evolutionary cycling, and is therefore incomplete with respect to determining the evolutionary dynamics of competitive interactions.

The existence of periodic orbits in the evolution of exploiter-victim interactions, such as predator-prey, parasite-host or plant-herbivore, also constitutes Red Queen evolution on the 'gene-frequency' time scale of Stenseth and Maynard-Smith (1984). The nature of those ecological interactions, however, gives a higher probability that such evolutionary dynamics will exist. This is due to the fact that the encounters are of ecological + / - type,

i.e. positive for one of the individuals (the predator) but negative for the other (prey). The adaptive evolutionary effects of this encounter will therefore be of opposite impacts; a change in the adaptive trait with positive effect for the one would constitute a deterioration of the biotic environment for the other. Competition is of true - / - type, where both individuals have a negative fitness effect of the encounter, and a small phenotypic mutation will in the case of symmetry change the impacts similarly for both populations. This is however not necessarily the case for asymmetric competition (even though it still constitutes an ecological - / - interaction), where an adaptive change in one species might deteriorate the biotic environment of the competitor. This can be understood as a more general reason for asymmetric competition leading to cycles or evolutionary arms races.

All identified limit cycles occurred when there was a difference in the evolutionary rates of the two competing populations. Even though it is impossible to state that periodic attractors of phenotypic evolution only will occur if one has a difference in the evolutionary rates of the competing populations, the analysis here in addition to that of Law et al. (1997) at least clearly indicates that it is by far more plausible with such a difference. Different evolutionary rates would typically be the case in natural systems where competitors are phylogenetically more distant. This is because they then may have a higher probability of having different life-histories and thus rates of evolution.

To evaluate the dynamics of this model in a more thorough way, one could utilize the tools of numerical bifurcation analysis to precisely define the parts of parameter-space that exhibits limit cycles. Such analysis of other adaptive dynamics models has been done to a certain extent in predator-prey systems (Marrow et al. 1992, Dercole et al. 2003) but not in models of competition. It remains clear though that while this type of dynamics is not predominant, it is still a possible outcome.

4.2 The limitations of the model.

One major drawback of the model is the separation of timescales, and the use of equilibrium population sizes in the invasion fitness. This separation is most probably not met in any evolutionary system, but there is another complication for the investigation of

asymmetric competition. Asymmetric competition can be dependent on the densities of the competing populations, with higher asymmetry when the densities are high, for instance in the case of asymmetric competition for light in plants. In the model presented here, asymmetries are the same regardless of densities, but one could argue that equilibrium population sizes correspond to high densities, and in that case the model is applicable if the selection occurs mainly at high densities. A more general interpretation would be that to evaluate the evolutionary dynamics of a competition system like the one under investigation, the methods should not include such a separation and take into account the density-dependence of asymmetry.

Most evolutionary models of any kind do not take the spatiality of nature into account, and that is not done here either. The mean-field assumption is made in all the models. This could fairly easily be lifted in the individual-based model by introducing a spatial dimension, where all individuals reside on a one- or two dimensional spatial scale, and by accounting the distance into the effect of competition. It is difficult to predict the effect this inclusion of spatiality could have on the dynamics, but in the simplest of scenarios, where there are only one evolutionary attractor, one would expect that the system eventually came to a halt at this attractor. Limit cycles in such a spatial system could take very different forms, and have different spatial dynamics. A model where one varied the size of the interaction neighborhood would be instructive in evaluating if there would be a larger subset of the parameters that would lead to such dynamics.

4.3 Concluding remarks – prevalence of Red Queen dynamics.

The deterministic model presented yielded several points in parameter-space with existence of limit cycles, and both the monomorphic stochastic and polymorphic stochastic representations of the system also portrayed such dynamics, thus substantiating the approximation. The subset of the parameter-space giving rise to cycles were fairly narrow, and it can be stated that the probabilities for ecological interactions as defined here amounting to continual evolution are comparably low. Limit cycles was however never experienced with no asymmetry in the interactions, and neither without any difference in evolutionary rates. The nature of competition in natural communities is most probably not symmetric, and competing species need not have equal rates of

evolution. Accordingly, these prerequisites for continual evolution are probably often satisfied. However, natural systems where the degree of asymmetry is larger in inter-specific interactions compared to intra-specific are probably seldom.

I did not assess the possible existence of Red Queen dynamics of branching-extinction type (Kisdi et al. 2001). However, the prevalence of branching points in the two-population model constitutes one of the prime conditions for such dynamics to occur.

Limit cycles in adaptive dynamics models of two-species with one evolvable trait, can be forced through scaling of the evolutionary rates if an equilibrium of the system can be characterized by convergence stability of one species, and that the off-diagonal elements in the Jacobian also are of opposite signs. This adds another analytical tool that can be utilized in adaptive dynamics models, and the characterization of non-stationary outcomes of phenotypic evolution in such models.

5. Appendices.

Appendix 1. The individual-based model.

The development of the individual-based model was based on earlier such models used in the adaptive dynamics literature (Dieckmann 1996), but in essence akin to any individual-based model.

The model is implemented using super-individuals, meaning that each unique trait-value in the system at any time is logged as the trait-value and the number of individuals of that trait value. This decreases computing time considerably. The model is initiated with two arrays representing the two populations;

$S_i = [[s_{i,j}, n_{i,j}], \ldots, [s_{i,u}, n_{i,u}]]$ for $i = 1,2$ and $j = 1..u$, where u are the number of unique trait-values in population i.

Then one defines the phenotypic distribution $P_i(s)$ for each population i as:

$$P_i(s) = \sum_{j=1}^{n_{i,u}} n_{i,j} \cdot Dirac(s - s_{i,j})$$

The Dirac delta function is defined as zero everywhere except for $Dirac(0)$ where it has a singularity and it has the property that

$$\int_{-\infty}^{\infty} Dirac(x) = 1$$

Then one calculates the transition probabilities for every (super-) individual j in both populations i, by mapping the trait-values into probabilities for a birth event and death event;

$$b_{i,j} = \beta_i \cdot n_{i,j}$$

$$d_{i,j} = \left(\delta(s_{i,j}) + \sum_{h=1}^{2} \int_{s=-\infty}^{\infty} c_{i,h} \cdot \alpha(s_{i,j} - s, k_{i,h}) \cdot P_h \right) \cdot n_{i,j}$$

$$w_{i,j} = b_{i,j} + d_{i,j}$$

where alpha and delta-functions are as defined in the main text. The $b_{i,j}$ and $d_{i,j}$ are not true probabilities unless they are scaled, because they can take values above 1. Also note that the sums would be different if the cost-function were to represent reduced fecundity, it is here taken to increase mortality risk, as it is part of $d_{i,j}$.

Then one calculates the total event-probabilities for each population (w_i) and the total event-probability (W) in the system;

$$w_i = \sum_{j=1}^{n_{i,u}} w_{i,j}$$

$$W = \sum_{i=1}^{2} w_i$$

Then a waiting time for the next event is drawn;

$$\Delta t = \left(-\frac{1}{W} \right) \cdot \ln(o)$$

where o is a number between 0 and 1 drawn from a uniform distribution. At the start of the simulation t is set to 0 and updated for every event.

For every iteration a population is drawn from the distribution of event-probabilities, [w_1/W, w_2/W], and then a (super-) individual from that selected population is drawn from the event-probabilities within that population [$w_{i,j}...w_{i,u}$]. Having selected an individual a particular event is implemented with probabilities calculated for that specific individual [$b_{i,j}/w_{i,j}$, $d_{i,j}/w_{i,j}$]. If the event drawn is a death-event the individual is taken out of the array (or the number of individuals with that particular trait-value is reduced by 1). If the event is a birth event, a mutation event is implemented with a certain probability (μ_i), or the number of individuals with the trait-value is increased by 1. A mutation is drawn from a normal distribution with variance σ_i and mean 0. For every event time t is updated and then all probabilities are recalculated. This is iterated for a predefined number of events or time.

The model was implemented in Maple (Maplesoft. 2003) and simulations where very time-consuming, which is reflected in the number of simulations performed. The trait-values for every 50th event were logged.

Appendix 2. The monomorphic stochastic model.

The monomorphic stochastic model can be described by a master equation in the following way;

$$\frac{d}{dt}P(s,t) = \int \left[w(s \mid s',t) \cdot P(s',t) - w(s' \mid s,t) \cdot P(s,t) \right] ds'$$

where $\boldsymbol{s}$ denotes the vector of trait-values (and $\boldsymbol{s}'$ denotes the vector of possible transitions), and $w(s' \mid s,t)$ denotes the probabilities per unit time for the transition $s \rightarrow s'$ at time t. $P(s,t)$ is the probability density of resident trait-values. As developed in Dieckmann (1996) in the infinitesimal time dt only transitions in one population have a nonvanishing probability per unit time;

$$w(s' \mid s) = \sum_{i=1}^{n} w_i(s'_i, s) \cdot \prod_{\substack{j=1 \\ j \neq i}}^{n} Dirac(s'_j - s)$$

In our case $n = 2$ and the expression is fairly simple. The derivation of the transition probability per unit time is derived in Dieckmann (1996) and can be expressed;

$$w_i(s'_i, s) = \mu_i(s_i) \cdot b_i(s_i, s) \cdot \hat{N}_i(s) \cdot M_i(s_i, s'_i - s_i) \cdot b_i^{-1}(s'_i, s) \cdot f_i(s'_i, s) \cdot Heaviside(f_i(s'_i, s))$$

where

$$M(s_i, s'_i - s_i) = \frac{\exp\left(-\frac{(s_i - s'_i)^2}{2 \cdot \sigma_i^2} \right)}{\sqrt{2 \cdot \pi \cdot \sigma_i^2}}$$

Here $\mu_i(s_i)$ is the mutation-rate (in our model independent of the trait-value), $b_i(s_i,s)$ is the probability for birth in population i given trait-vector $\boldsymbol{s}$, $\hat{N}_i(s)$, equilibrium population sizes, $M_i(s_i,s_i'-s_i)$ is the mutation distribution (i.e. the distribution of probabilities of trait-value s_i giving rise to trait-value s_i') and $f_i(s_i',\boldsymbol{s})$ is the invasion-fitness of s_i' in a

community defined by ***s***. The use of the Heaviside function is to map negative invasion-fitnesses to zero.

The implementation of the model is straightforward; first one initiates the model with two populations with one unique trait-value each, sets t=0 and specifies t_{end}, the time for the simulation to end. Then one calculates the event-probabilities for each population and the total;

$$w_i = \int w_i(s_i', s)ds_i' \qquad\qquad w = \sum_{i=1}^{n} w_i$$

Then a waiting time is chosen as in the individual based model, and a population is chosen with probability $\frac{1}{w} \cdot w_i$. The new trait-value for this population is chosen from the distribution $\frac{1}{w_i} \cdot w_i(s_i', s)$. Then time and ***s*** is updated and the procedure is continued until t_{end}. This was also implemented using Maple (Maplesoft. 2003).

Appendix 3. Derivation of the criteria for Hopf-bifurcations.

Assume that we have located an equilibrium of the dynamical system. The linearization (i.e. Jacobian) around the point will yield the asymptotic behavior of the system in the vicinity of that point. We can write the Jacobian;

$$Let: \frac{d}{dt} s_i(t) = \kappa_i(s) \cdot \frac{\partial}{\partial s_{mut|i}} f_i(s_{mut|i}, s)$$

$$Then: \mathbf{J} = \begin{bmatrix} \kappa_1(s) \cdot \frac{\partial}{\partial s_1}\left[\frac{\partial}{\partial s_{mut|1}} f_1(s_{mut|1}, s)\right] & \kappa_1(s) \cdot \frac{\partial}{\partial s_2}\left[\frac{\partial}{\partial s_{mut|1}} f_1(s_{mut|1}, s)\right] \\ \kappa_2(s) \cdot \frac{\partial}{\partial s_1}\left[\frac{\partial}{\partial s_{mut|2}} f_2(s_{mut|2}, s)\right] & \kappa_2(s) \cdot \frac{\partial}{\partial s_2}\left[\frac{\partial}{\partial s_{mut|2}} f_2(s_{mut|2}, s)\right] \end{bmatrix}$$

The diagonal elements can be shown to correspond to the criteria for convergence stability for the two populations (Abrams et al. 1993b, Marrow et al. 1996).

The point is an attractor if *tr (J) < 0* and *det(J) > 0*, thus convergence of both populations is not sufficient conditions for dynamic stability because even if *tr(J) <0*, *det(J)* might still be less than zero. If the point is lacking convergence stability for both populations

(i.e. *tr(J) > 0*), it will be an evolutionary repellor. If the point is convergence stable for both populations and the off-diagonal elements are of opposite signs the point will be an attractor. If the point is convergence stable for only one population, and the off-diagonal elements are of same sign, it will be a repellor (*det(J) < 0*).

The system can be both locally stable and unstable if only one of the population is convergence stable if *det(J)>0*, since *tr(J)* can be of both signs. This corresponds to weak convergence stability of Leimar (2002). In this case the system can be forced through a Hopf-bifurcation by scaling the parameters in the κ-functions as shown below.

For the system to undergo a Hopf-bifurcation, the eigenvalues must (as one varies on parameter) change from having non-zero imaginary part and negative real-part (meaning that it is a spiral sink) to having non-zero imaginary part and positive real-part (meaning that it is a spiral source). In this range there must exist a point where the eigenvalues are pure imaginary, and this constitutes a Hopf-bifurcation point.

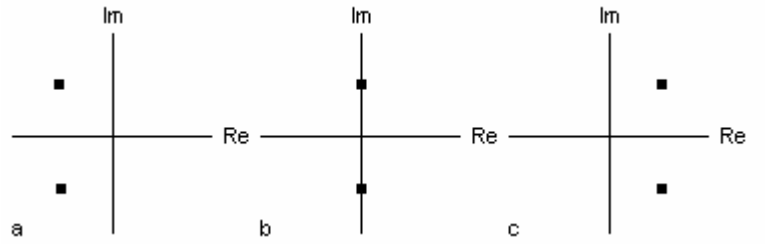

Figure A.1. Plots showing the eigenvalues of the Jacobian evaluated at a dynamical equilibrium, where the axis represent the imaginary (Im) and the real part (Re). a correspond to a spiral sink, c to a spiral source and b to the exact bifurcation point.

$$Let: a = \frac{\partial}{\partial s_1}\left[\frac{\partial}{\partial s_{mut|1}} f_1\left(s_{mut|1}, s\right)\Big|_{S_{mut|1}=s}\right], b = \frac{\partial}{\partial s_2}\left[\frac{\partial}{\partial s_{mut|1}} f_1\left(s_{mut|1}, s\right)\Big|_{S_{mut|1}=s}\right],$$

$$c = \frac{\partial}{\partial s_1}\left[\frac{\partial}{\partial s_{mut|2}} f_2\left(s_{mut|2}, s\right)\Big|_{S_{mut|2}=s}\right], d = \frac{\partial}{\partial s_1}\left[\frac{\partial}{\partial s_{mut|2}} f_2\left(s_{mut|2}, s\right)\Big|_{S_{mut|2}=s}\right]$$

Then;

$$\mathbf{J} = \begin{bmatrix} \kappa_1(s)\cdot a & \kappa_1(s)\cdot b \\ \kappa_2(s)\cdot c & \kappa_2(s)\cdot d \end{bmatrix} = \mathbf{ML}, \textit{where}$$

$$\mathbf{M} = \begin{bmatrix} \kappa_1(s) & 0 \\ 0 & \kappa_2(s) \end{bmatrix} \quad \textit{and} \quad \mathbf{L} = \begin{bmatrix} a & b \\ c & d \end{bmatrix}$$

For there to be some part of the space defined by the parameters in the κ-function (or the 'mutational matrix', ***M***) where a Hopf-bifurcation occurs, we need that there is some range where the eigenvalues of the Jacobian can take all constellations shown in figure A.1. Remember that as we change the parameters in the κ-functions, the positioning of the evolutionary isoclines, and thus the positioning of the equilibrium does not change. This also means that *a, b, c* and *d* in the Jacobian above does not change (i.e. $det(\mathbf{L}) > 0$). To vary the κ-function, we need to vary the mutation rate or mutational variance of one of the populations, as the equilibrium population sizes will be constant for the same equilibrium body sizes. Also remember the conditions; *a* and *d* of opposite signs and $det(\mathbf{L})>0$ (i.e. *b* and *c* also of opposite signs and sufficient size). For the eigenvalues of the Jacobian (***J***) at the point to have non-zero imaginary parts we need (for notation the dependence on *s* is left out since at the evolutionary equilibrium point the equilibrium population sizes will be constant as we vary μ_i or σ_i);

$$\left(\kappa_1 \cdot a - \kappa_2 \cdot d\right)^2 + 4 \cdot \kappa_1 \cdot \kappa_2 \cdot b \cdot c < 0 \qquad \text{(A.I)}$$

Since we are interested in the scaling of κ's, let $\rho = \kappa_1 / \kappa_2$. If we substitute for κ_1, we then obtain:

$$\kappa_2^{\,2} \cdot \left(a^2 \cdot \rho^2 + \left(4 \cdot b \cdot c - 2 \cdot a \cdot d\right) \cdot \rho + d^2\right) < 0 \qquad \text{(A.II)}$$

A necessary condition for A.II is:

$$\left(4 \cdot b \cdot c - 2 \cdot a \cdot d\right) < 0 \qquad \text{(A.III)}$$

since ρ only can take positive values. This will always hold, since *det(**J**)>0* implies *det(**M**)det(**L**)>0*, i.e. *det(**L**)>0* since ***M*** is symmetric and positive-definite. Thus will also be the sufficient condition.

To illustrate in a different way, assume we have found an equilibrium where *a* and *d* are of opposite signs, and *det(**J**)>0*. Then we can scale the mutation rate for one population such that the left hand side of A.II is the terms in the square-root of the eigenvalues. Let *g* be a function describing the terms under the square-root in the eigenvalues, i.e. the left hand side of A.II, as a function of $\rho = \kappa_1 / \kappa_2$. We can differentiate this function with respect to ρ to find its minimum, and whether this is negative;

$$g(\rho) = a^2 \cdot \rho^2 + \left(4 \cdot b \cdot c - 2 \cdot a \cdot d\right) \cdot \rho + d^2$$

$$g'(\rho) = 2 \cdot a^2 \cdot \rho + 4 \cdot b \cdot c - 2 \cdot a \cdot d = 0$$

$$\rho_{\min} = \frac{a \cdot d - 2 \cdot b \cdot c}{a^2}$$

$$g(\rho_{\min}) = \frac{4 \cdot b \cdot c \cdot \left(a \cdot d - b \cdot c\right)}{a^2}$$

We here see that the minimum value for the left hand side of A.II will be negative (yielding imaginary parts of the eigenvalues), since *det(**J**)= a d – b c > 0* (*b* and *c* of opposite signs). We also see that this will happen when $\rho > 0$.

To make sure that the system can undergo a Hopf-bifurcation in this subspace we need that the real part of the eigenvalues can shift from positive to negative within this region. If we substitute the boundary-values for ρ yielding non-zero imaginary parts (i.e. solutions of $g(\rho) = 0$ above), into the real parts of the eigenvalues we get;

$$\mathrm{Re}(\lambda) = \underbrace{\kappa_2 \cdot \left(d - \frac{b \cdot c}{a}\right)}_{I} \pm \underbrace{\kappa_2 \cdot \frac{\sqrt{-a \cdot d \cdot b \cdot c + b^2 \cdot c^2}}{a}}_{II} \qquad \text{(A.IV)}$$

For A.IV to take both negative and positive values, we need that the last term (II) is in absolute value larger than the absolute value of the first (I). This yields;

$$a \cdot d - b \cdot c > 0,$$

i.e.

$$\det(\mathbf{L}) > 0$$

So if a and d are of opposite signs, in addition to the criteria $det(\mathbf{L}) > 0$ (which implies b and c of opposite signs), then the system can be forced through a Hopf-bifurcation by scaling the evolutionary rates and a limit cycle will necessarily occur.

Appendix 4. Notation.

The following notation is used in the thesis;

Symbol/function	Interpretation
s_i	Trait-value of population/individual i. Without subscript denotes the vector of two trait-values. Also referred to as body size.
$s_{mut\|i}$	Trait-value of mutant appearing in population i.
Δs	Denoting the difference in trait-values.
$k_{i,j}$	Degree of asymmetry in the effect of the interaction between individual/population i and j on population i. Non-negative.
α - function	Function describing the effect of the competitive interaction
δ - function	Function describing the mortality dependent on the trait-value.
c_1, c_2, c_3	Parameters of the δ – function. All positive.
β_i	Birth rate of population i. All positive.
N_i	Size of population i. Dependent either on time and the vector of trait-values or only the trait-values when dealing with equilibrium population sizes, $\hat{N}$.
$c_{i,j}$	Parameter that scale the interaction between population i and j.
μ_i	Mutation-rate in population i.
σ_i^2	Mutational variance in population i.
κ- function	The function scaling the evolutionary rate, dependent on the vector of trait-values, as it includes population size.

Cited literature:

Abrams, P. A., Y. Harada, and H. Matsuda. 1993a. On the relationship between quantitative genetic and ess models. Evolution **47**:982-985.

Abrams, P. A., and H. Matsuda. 1994. The evolution of traits that determine ability in competitive contests. Evolutionary Ecology **8**:667-686.

Abrams, P. A., and H. Matsuda. 1997a. Fitness minimization and dynamic instability as a consequence of predator-prey coevolution. Evolutionary Ecology **11**:1-20.

Abrams, P. A., and H. Matsuda. 1997b. Prey adaptation as a cause of predator-prey cycles. Evolution **51**:1742-1750.

Abrams, P. A., H. Matsuda, and Y. Harada. 1993b. Evolutionarily Unstable Fitness Maxima and Stable Fitness Minima of Continuous Traits. Evolutionary Ecology **7**:465-487.

Alatalo, R. V., and J. Moreno. 1987. Body size, interspecific interactions, and use of foraging sites in tits (Paridae). Ecology **68**:1773-1777.

Alroy, J. 1996. Constant extinction, constrained diversification, and uncoordinated stasis in North American mammals. Palaeogeography Palaeoclimatology Palaeoecology **127**:285-311.

Alroy, J., P. L. Koch, and J. C. Zachos. 2000. Global climate change and North American mammalian evolution. Paleobiology **26**:259-288.

Barnosky, A. D. 2001. Distinguishing the effects of the Red Queen and Court Jester on Meiocene mammal evolution in the northern Rocky Mountains. Journal of Vertebrate Paleontology **21**:172-185.

Bowers, R. G., A. White, M. Boots, S. A. H. Geritz, and E. Kisdi. 2003. Evolutionary branching/speciation: contrasting results from systems with explicit or emergent carrying capacities. Evolutionary Ecology Research **5**:883-891.

Carroll, L. 1872. Through the looking glass.

Christiansen, F. B. 1991. On conditions for evolutionary stability for a continuously varying character. American Naturalist **138**:37-50.

Cluttonbrock, T. H., S. D. Albon, R. M. Gibson, and F. E. Guinness. 1979. Logical stag - Adaptive aspects of fighting in red deer (Cervus-Elaphus L). Animal Behaviour **27**:211-225.

Connell, J. H. 1983. On the prevalence and relative importance of interspecific competition - Evidence from field experiments. American Naturalist **122**:661-696.

Dawkins, R., and J. R. Krebs. 1979. Arms Races Between And Within Species. Proceedings of the Royal Society of London Series B-Biological Sciences **205**:489-511.

Dercole, F. 2003. Remarks on branching-extinction evolutionary cycles. Journal of Mathematical Biology **47**:569-580.

Dercole, F., J. O. Irisson, and S. Rinaldi. 2003. Bifurcation analysis of a prey-predator coevolution model. Siam Journal on Applied Mathematics **63**:1378-1391.

Dieckmann, U. 1996. The dynamical theory of coevolution. Ph.D thesis. Leiden University, Leiden.

Dieckmann, U., and M. Doebeli. 1999. On the origin of species by sympatric speciation. Nature **400**:354-357.

Dieckmann, U., and R. Law. 1996. The dynamical theory of coevolution: A derivation from stochastic ecological processes. Journal of Mathematical Biology **34**:579-612.

Dieckmann, U., P. Marrow, and R. Law. 1995. Evolutionary cycling in predator-prey interactions - Population-dynamics and the Red Queen. Journal of Theoretical Biology **176**:91-102.

Doebeli, M., and U. Dieckmann. 2000. Evolutionary branching and sympatric speciation caused by different types of ecological interactions. American Naturalist **156**:S77-S101.

Eshel, I. 1983. Evolutionary and continuous stability. Journal of Theoretical Biology **103**:99-111.

Eshel, I., and U. Motro. 1981. Kin selection and strong evolutionary stability of mutual help. Theoretical Population Biology **19**:420-433.

Farkas, M. 1994. Periodic motions. Springer-Verlag, New York.

Gandon, S. 2002. Local adaptation and the geometry of host-parasite coevolution. Ecology Letters **5**:246-256.

Gavrilets, S. 1997. Coevolutionary chase in exploiter-victim systems with polygenic characters. Journal of Theoretical Biology **186**:527-534.

Geritz, S. A. H., and E. Kisdi. 2000. Adaptive dynamics in diploid, sexual populations and the evolution of reproductive isolation. Proceedings of the Royal Society of London Series B-Biological Sciences **267**:1671-1678.

Geritz, S. A. H., E. Kisdi, G. Meszena, and J. A. J. Metz. 1998. Evolutionarily singular strategies and the adaptive growth and branching of the evolutionary tree. Evolutionary Ecology **12**:35-57.

Geritz, S. A. H., J. A. J. Metz, E. Kisdi, and G. Meszena. 1997. Dynamics of adaptation and evolutionary branching. Physical Review Letters **78**:2024-2027.

Iwasa, Y., and A. Pomiankowski. 1991. The Evolution Of Costly Mate Preferences.2. The Handicap Principle. Evolution **45**:1431-1442.

Kisdi, E. 1999. Evolutionary branching under asymmetric competition. Journal of Theoretical Biology **197**:149-162.

Kisdi, E., and S. A. H. Geritz. 2001. Evolutionary disarmament in interspecific competition. Proceedings of the Royal Society of London Series B-Biological Sciences **268**:2589-2594.

Kisdi, E., and S. A. H. Geritz. 2003. Competition-colonization trade-off between perennial plants: exclusion of the rare species, hysteresis effects and the robustness of co-existence under replacement competition. Evolutionary Ecology Research **5**:529-548.

Kisdi, E., F. J. A. Jacobs, and S. A. H. Geritz. 2001. Red Queen evolution by cycles of evolutionary branching and extinction. Selection **2**:161-176.

Kisdi, E., and S. Liu. 2006. Evolution of handling time can destroy the coexistence of cycling predators. Journal of Evolutionary Biology **19**:49-58.

Kisdi, T. 2004. Optimal body size, density-dependent selection gradients, and phenotypic variance under asymmetric competition. Ecology **85**:1460-1467.

Law, R., P. Marrow, and U. Dieckmann. 1997. On evolution under asymmetric competition. Evolutionary Ecology **11**:485-501.

Lawton, J. H., and M. P. Hassell. 1981. Asymmetrical Competition In Insects. Nature **289**:793-795.
Leimar, O. 2002. Multidimensional convergence stability and the canonical adaptive dynamics. *in* U. Dieckmann and J. A. J. Metz, editors. Elements of Adaptive Dynamics. Cambridge University Press, Cambridge.
Loeuille, N., M. Loreau, and R. Ferriere. 2002. Consequences of plant-herbivore coevolution on the dynamics and functioning of ecosystems. Journal of Theoretical Biology **217**:369-381.
Maplesoft. 2003. Maple 9.00. *in*. Maplesoft, Waterloo Maple Inc.
Marrow, P., U. Dieckmann, and R. Law. 1996. Evolutionary dynamics of predator-prey systems: An ecological perspective. Journal of Mathematical Biology **34**:556-578.
Marrow, P., R. Law, and C. Cannings. 1992. The coevolution of predator prey interactions - ESSs and Red Queen dynamics. Proceedings of the Royal Society of London Series B-Biological Sciences **250**:133-141.
Martins, J. S. S. 2000. Simulated coevolution in a mutating ecology. Physical Review E **61**:R2212-R2215.
Matsuda, H., and P. A. Abrams. 1994. Runaway Evolution To Self-Extinction Under Asymmetrical Competition. Evolution **48**:1764-1772.
Metz, J. A. J., R. M. Nisbet, and S. A. H. Geritz. 1992. How should we define fitness for general ecological scenarios. Trends in Ecology & Evolution **7**:198-202.
Morin, P. J., and E. A. Johnson. 1988. Experimental Studies Of Asymmetric Competition Among Anurans. Oikos **53**:398-407.
Parker, G. A. 1983. Arms Races In Evolution - An Ess To The Opponent-Independent Costs Game. Journal of Theoretical Biology **101**:619-648.
Persson, L. 1985. Asymmetrical Competition - Are Larger Animals Competitively Superior. American Naturalist **126**:261-266.
Raia, P., P. Piras, and T. Kotsakis. 2005. Turnover pulse or Red Queen? Evidence from the large mammal communities during the Plio-Pleistocene of Italy. Palaeogeography Palaeoclimatology Palaeoecology **221**:293-312.
Robinson, S. K., and J. Terborgh. 1995. Interspecific aggression and habitat selection by Amazonian birds. Journal of Animal Ecology **64**:1-11.
Schoener, T. W. 1983. Field experiments on interspecific competition. American Naturalist **122**:240-285.
Schwinning, S., and J. Weiner. 1998. Mechanisms determining the degree of size asymmetry in competition among plants. Oecologia **113**:447-455.
Stenseth, N. C., and J. Maynard-Smith. 1984. Coevolution in ecosystems - Red Queen evolution or stasis. Evolution **38**:870-880.
Taper, M. L., and T. J. Case. 1992. Models of Character Displacement and the Theoretical Robustness of Taxon Cycles. Evolution **46**:317-333.
Taylor, P. D. 1989. Evolutionary stability in one-parameter models under weak selection. Theoretical Population Biology **36**:125-143.
Van Valen, L. 1973. A new evolutionary law. Evolutionary Theory **1**:1-30.
Vrba, E. S. 1993. Turnover-pulses, the Red Queen, and related topics. American Journal of Science **293A**:418-452.
Waxman, D., and S. Gavrilets. 2005. 20 questions on adaptive dynamics. Journal of Evolutionary Biology **18**:1139-1154.

Webb, C. 2003. A complete classification of Darwinian extinction in ecological interactions. American Naturalist **161**:181-U181.
Weiner, J. 1990. Asymmetric Competition In Plant-Populations. Trends in Ecology & Evolution **5**:360-364.